

The challenge of simultaneously matching the diversity of chemical abundance patterns in cosmo hydro simulations

Tobias Buck

tbuck@aip.de

Leibniz-Institut für Astrophysik
Potsdam

Jan Rybizki,
Aura Obreja,
Andrea V. Macciò,
Melissa Ness,
Sven Buder,
Christoph Pfrommer,
Matthias Steinmetz

somewhere in cyber space,
30.6.2021

The challenge of simultaneously matching the diversity of chemical abundance patterns in cosmo hydro simulations

Tobias Buck

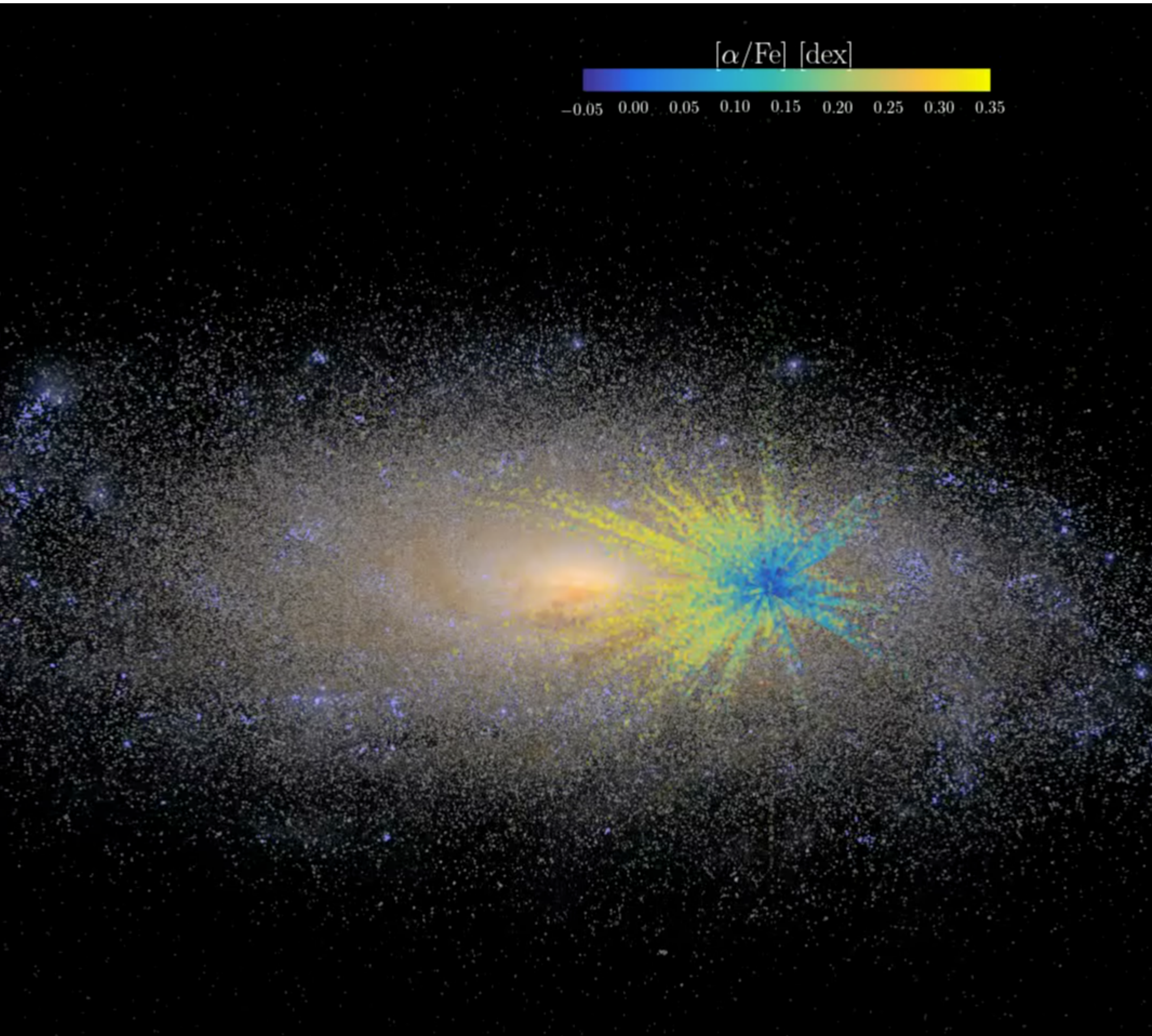
tbuck@aip.de

Leibniz-Institut für Astrophysik
Potsdam

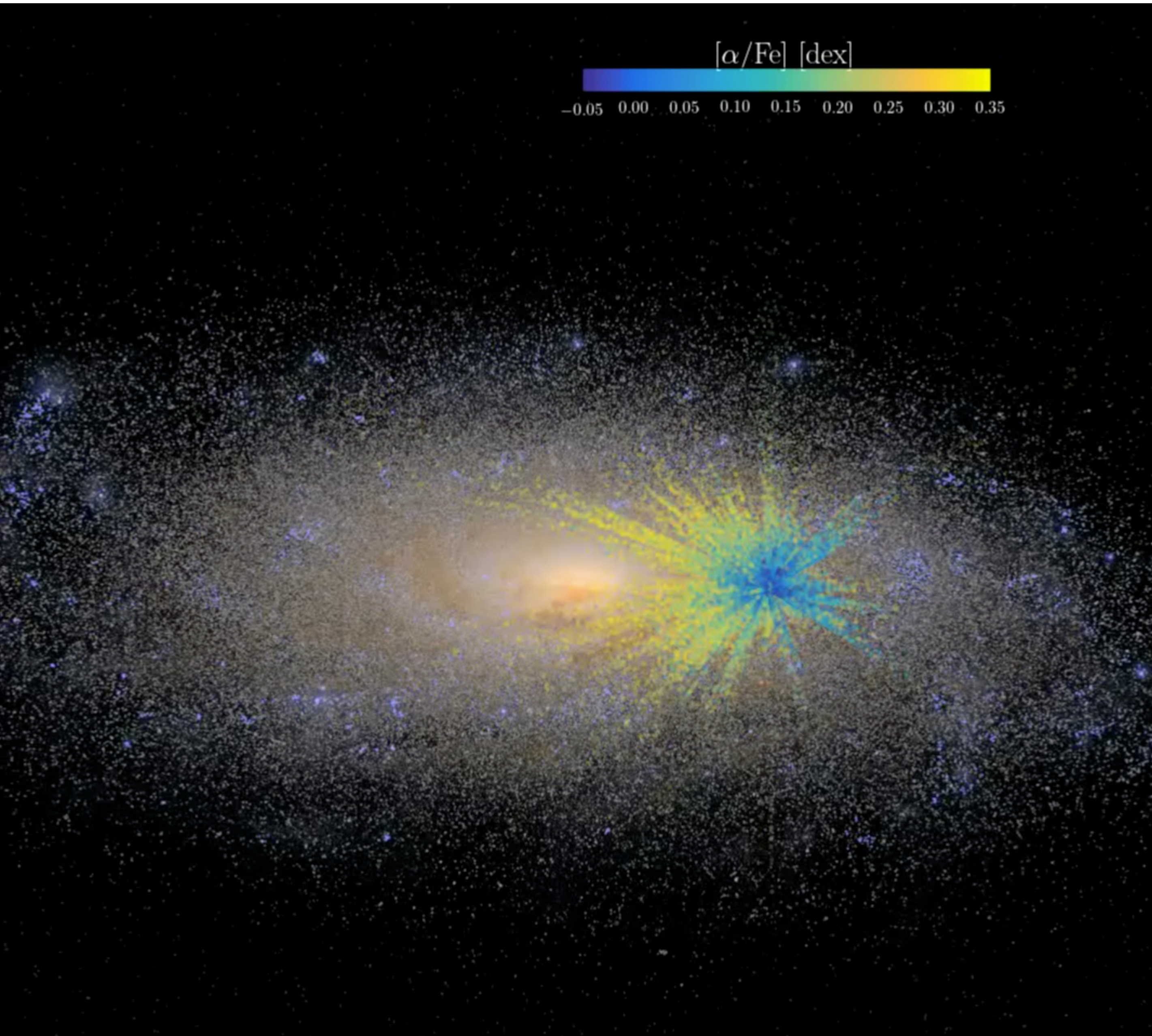
Jan Rybizki,
Aura Obreja,
Andrea V. Macciò,
Melissa Ness,
Sven Buder,
Christoph Pfrommer,
Matthias Steinmetz

somewhere in cyber space,
30.6.2021

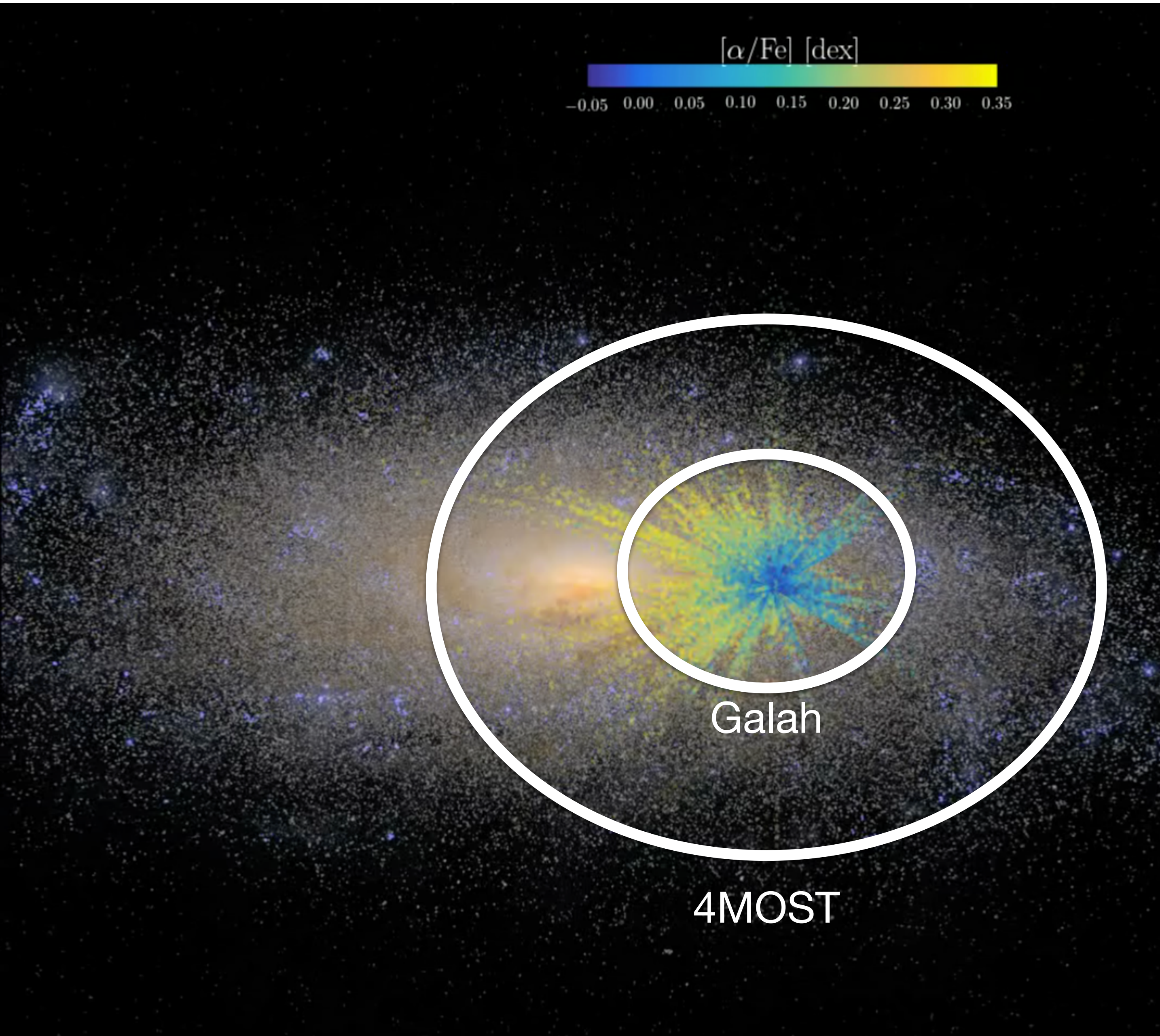
Milky Way chemo-dynamics: What we know



Milky Way chemo-dynamics: What we know



Milky Way chemo-dynamics: What we know

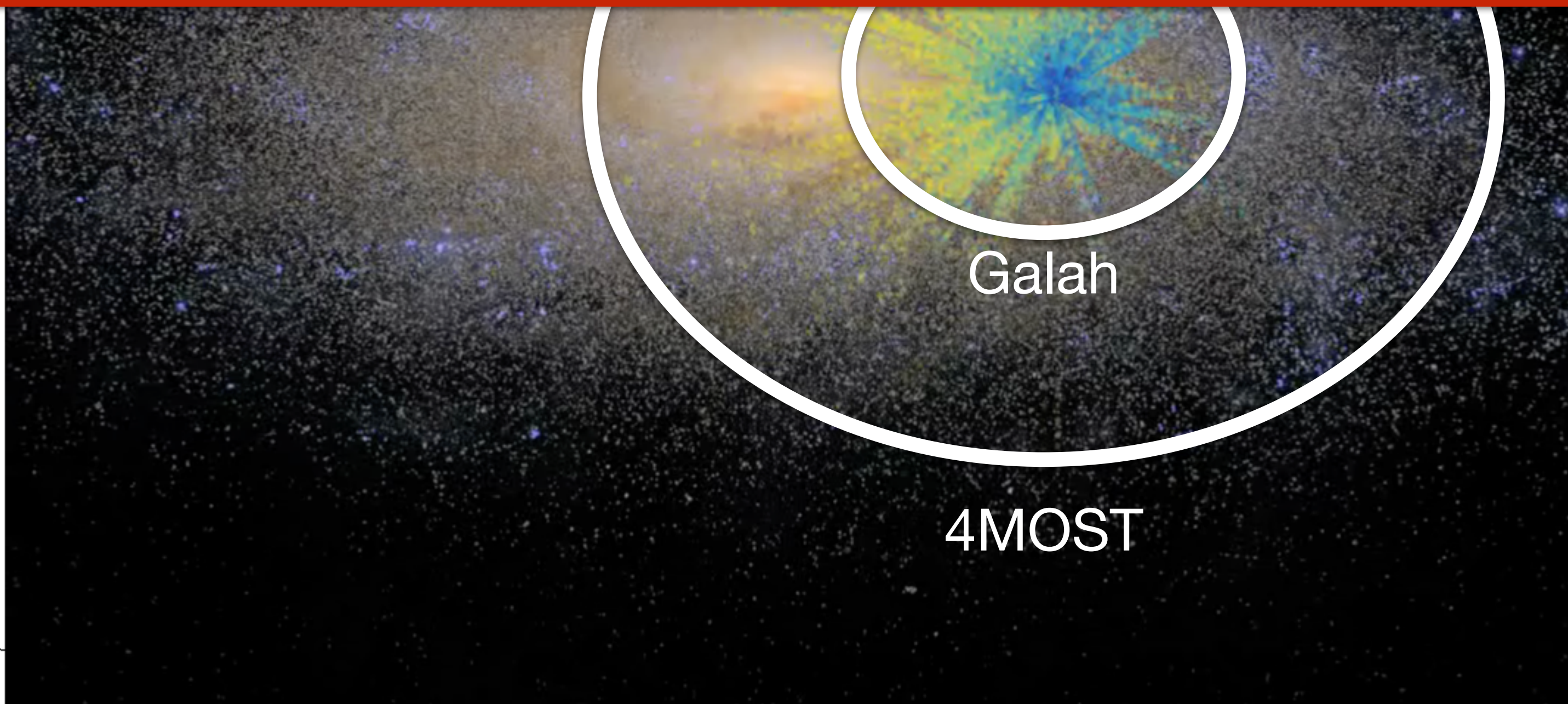


Animation based on
NIHAO-UHD simulations
(Buck+2020)

and Galah data
(Buder+2021)

Milky Way chemo-dynamics: What we know

Galah → 30 abundances
Gaia → precise kinematics
and abundances see M. Fouesneau Gaia talk
plus stellar ages
see the great talks of the morning session



Animation based on
NIHAO-UHD simulations
(Buck+2020)

and Galah data
(Buder+2021)

Milky Way chemo-dynamics: What we know

Galah → 30 abundances
Gaia → precise kinematics
and abundances see M. Fouesneau Gaia talk
plus stellar ages
see the great talks of the morning session

**What do these patterns tell us about
Milky Way's formation history?**

(based on
simulations
(Buder+2020))

and Galah data
(Buder+2021)



Estimating the Milky Way dark matter halo spin from observational data

Aura Obreja, et al.

Introduction

One important physical property of dark matter (DM) halos is the angular momentum J_h , or alternatively the spin λ which is an adimensional measure of J_h (Peebles 1969). In theory, a halo acquires its spin through tidal torques induced by the misalignments between the inertia tensor of the collapsing Lagrangian patch of the halo and the large scale tidal field (tidal torque theory, Hoyle 1951; Peebles 1969; Doroshkevich 1970; Fall & Efstathiou 1980; White 1984). In this scenario, most of the halo angular momentum is acquired in the high-z universe, where perturbations growth linearly. At later times,

Milky Way's thin and thick stellar disks

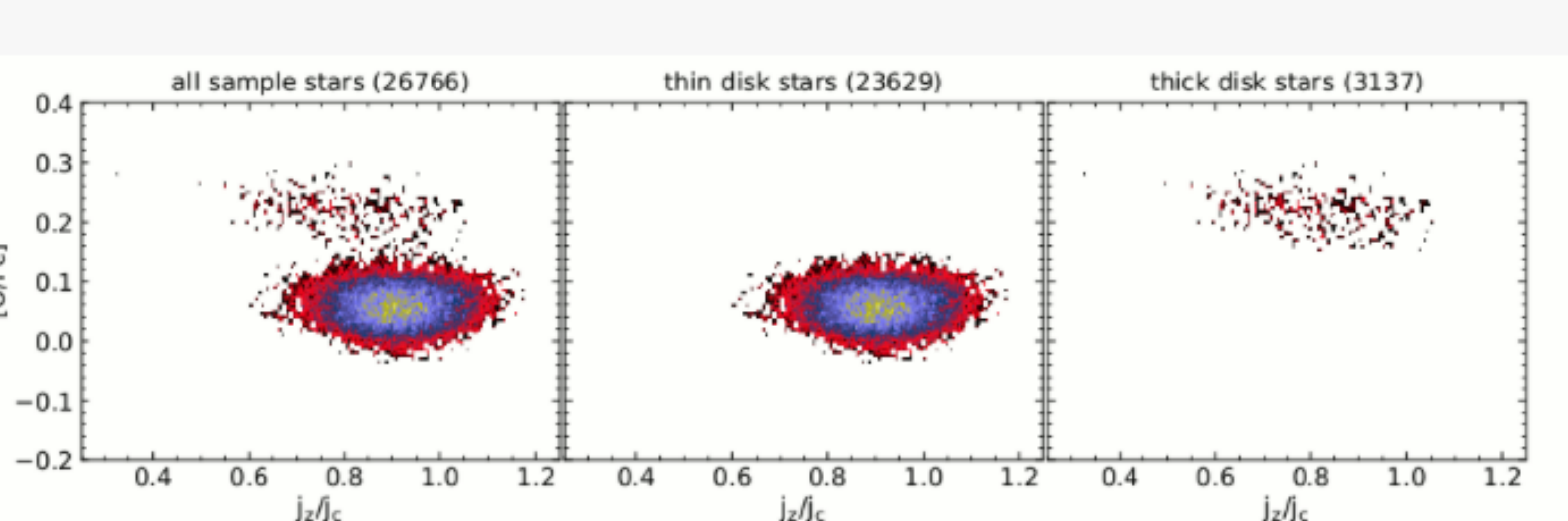


Fig. 3: MW disk separation in the feature space j_z/j_c - $[O/Fe]$ using the Gaussian Mixture clustering of scikit-learn with 2 components.

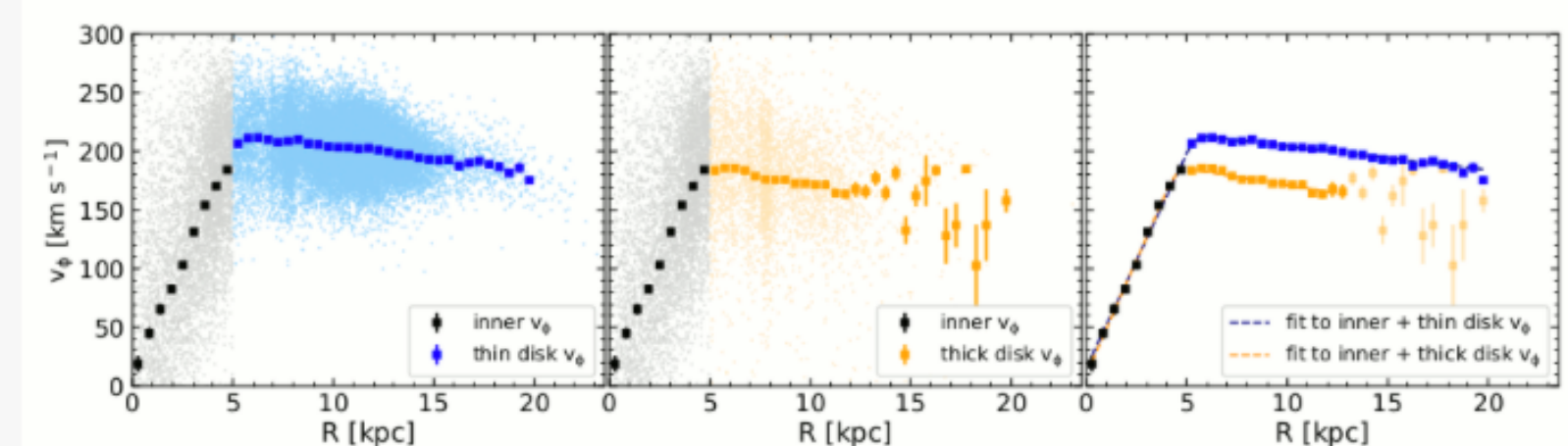
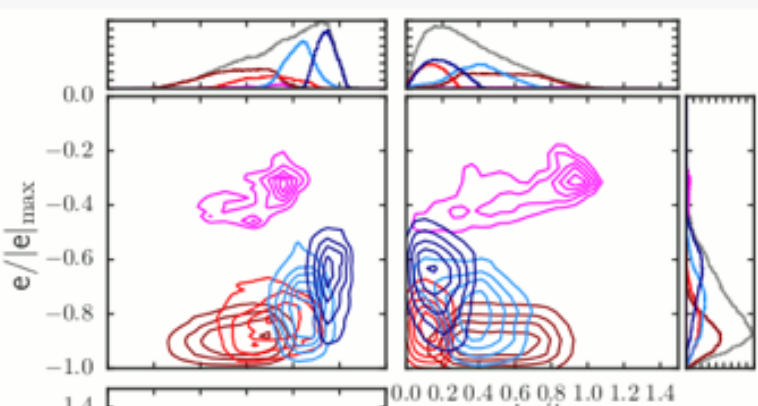


Fig. 4: $v_\phi(R)$ profiles for the thin (blue) and thick (orange) MW's disks. The grey points are stars with $|l| < 1$ kpc and $|v_\phi| < 350$ km/s, used to construct the inner $v_\phi(R)$ profile (black). The light blue/orange points are the thin/thick disk stars selected in the j_z/j_c - $[O/Fe]$ space.

To define the rotational velocities of the two stellar disks as function of radius $v_\phi(R)$, we use the

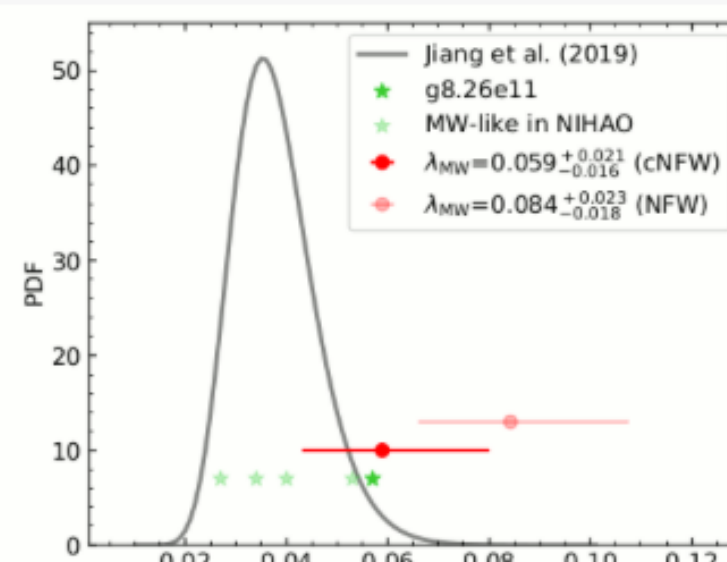
Galactic Structure Finder applied to NIHAO

In Obreja et al. (2019) we analyzed with GSF a sample of 25 NIHAO galaxies, and found eight types of stellar structures: large scale single disks, thin and thick disk, inner disks (~bars), spheroids, classical and pseudo bulges, and



The spin of Milky Way's DM halo

Using the derived total azimuthal angular momentum for MW's stellar disk J_z together with the relation between J_h and J_z , we estimate a value for the total angular momentum of the MW's DM halo $J_h = 2.57^{+0.34}_{-0.30} \times 10^{15} M_\odot \text{ kpc} \cdot \text{km} \cdot \text{s}^{-1}$ assuming the contracted NFW model (Cautun et al. 2020) $\lambda = 1.2 \text{ e}^{+0.40}_{-0.40}$



Aim:

Modify our cosmological numerical codes to keep up with the data quality and quantity of spectroscopic surveys

Star particles in cosmological simulations



Star particles in cosmological simulations

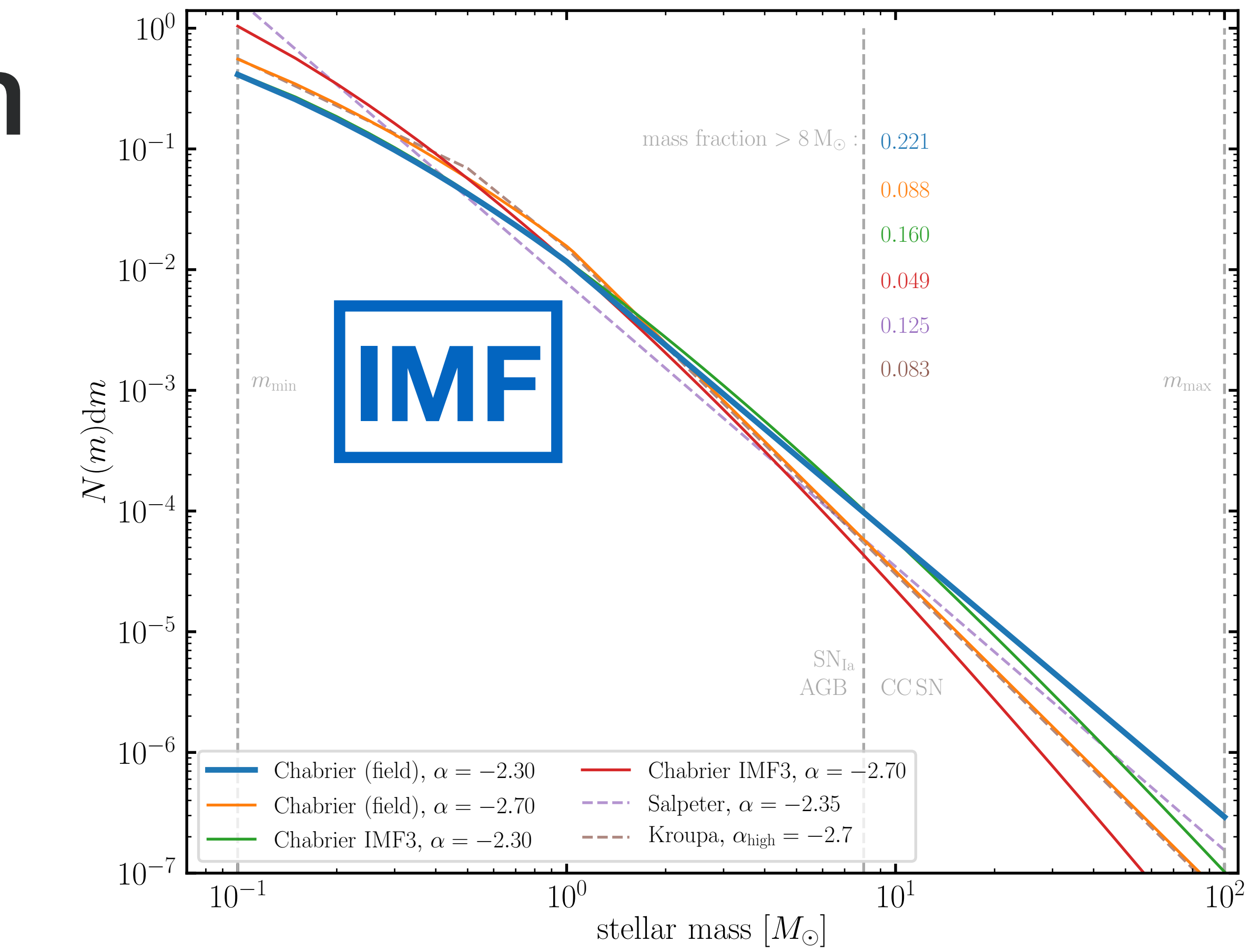
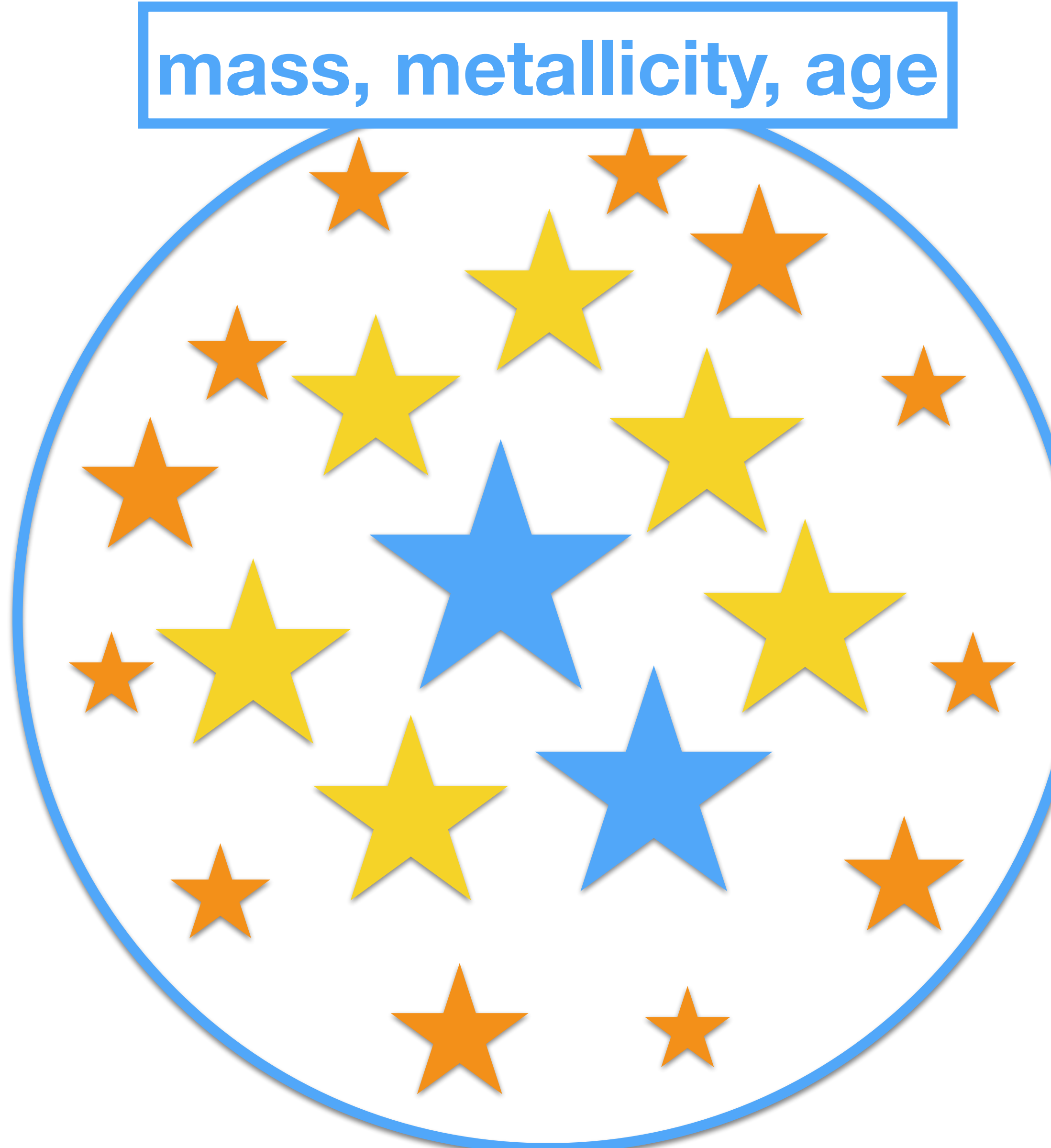


Simple stellar population

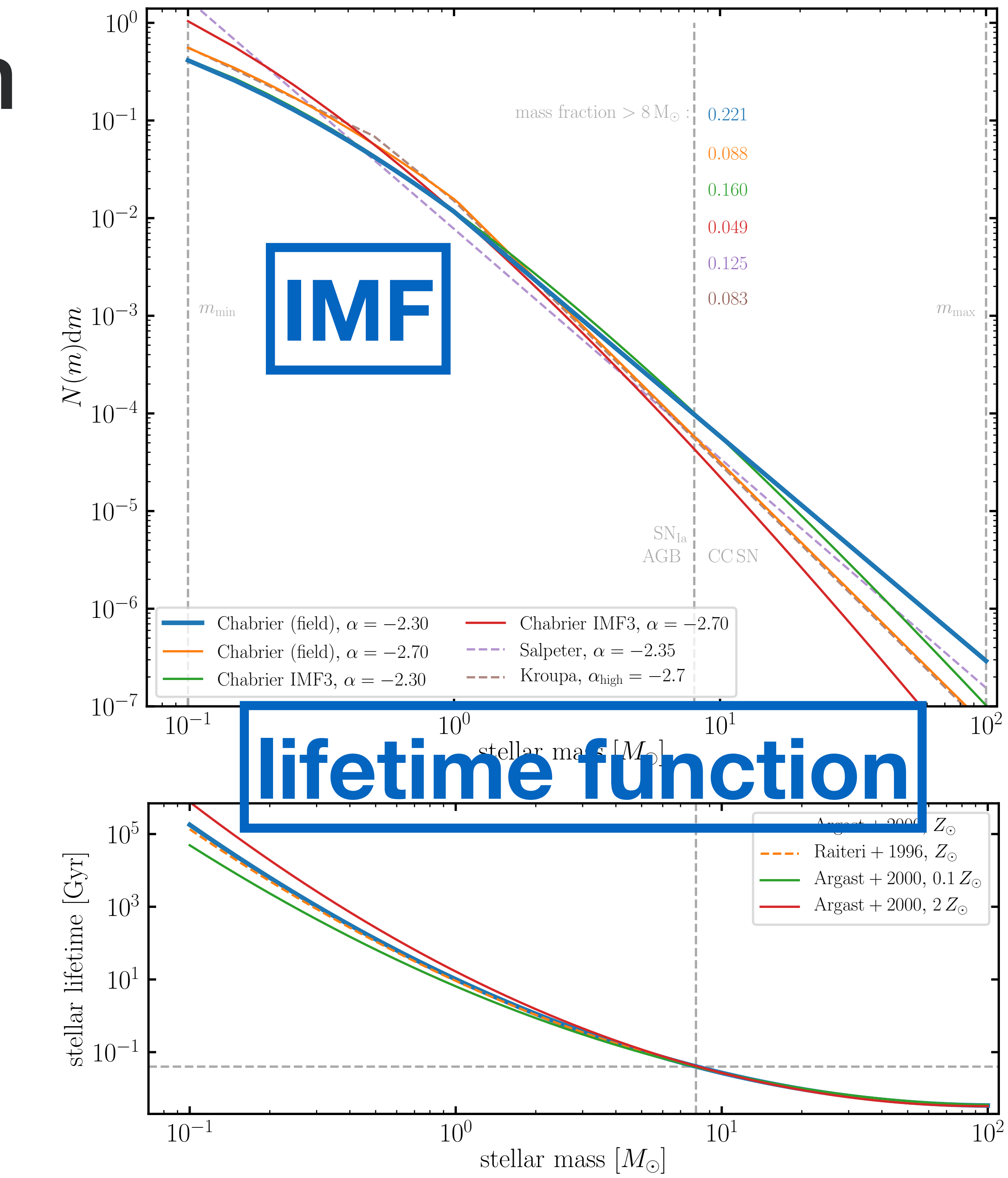
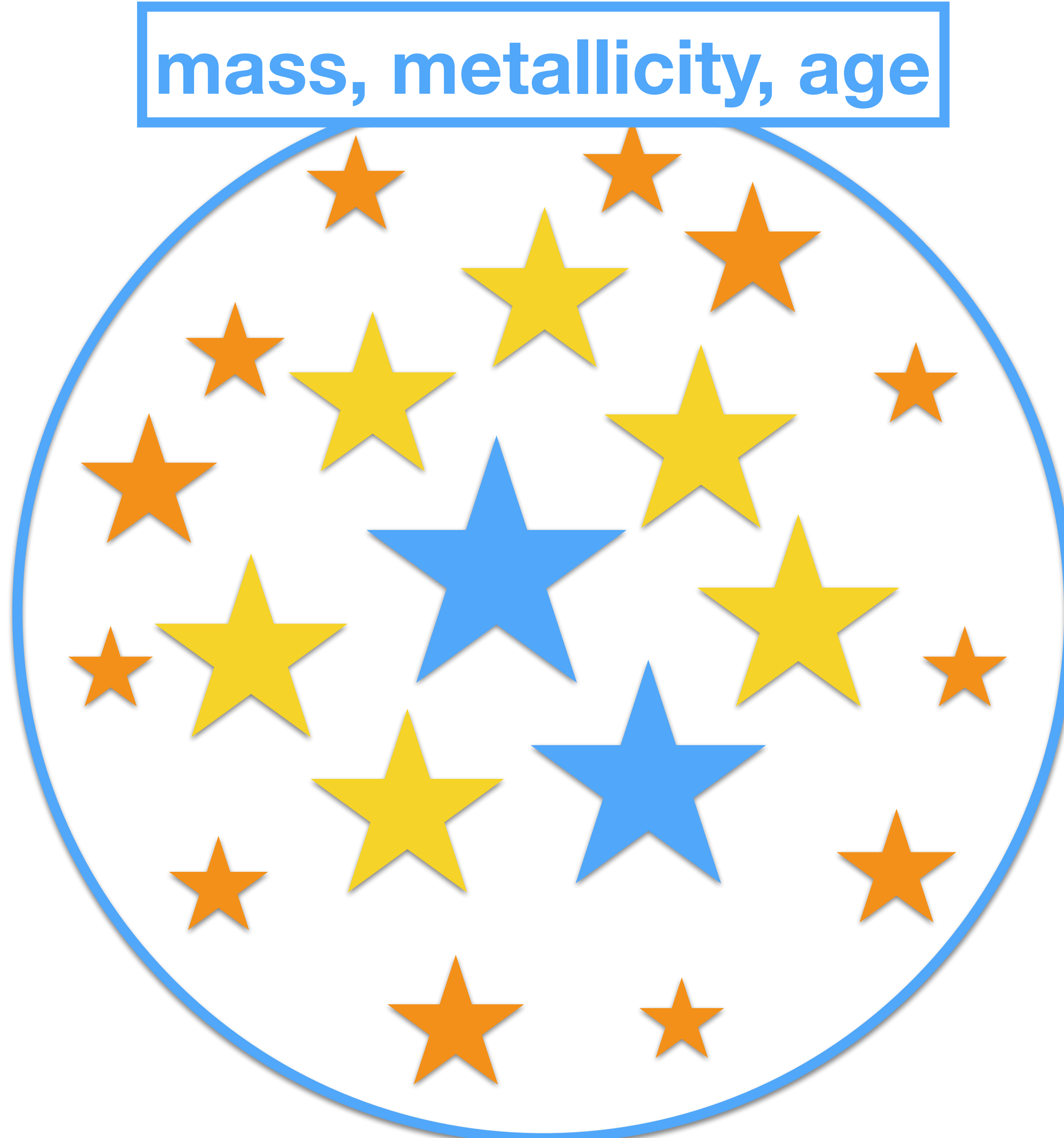
mass, metallicity, age



Simple stellar population

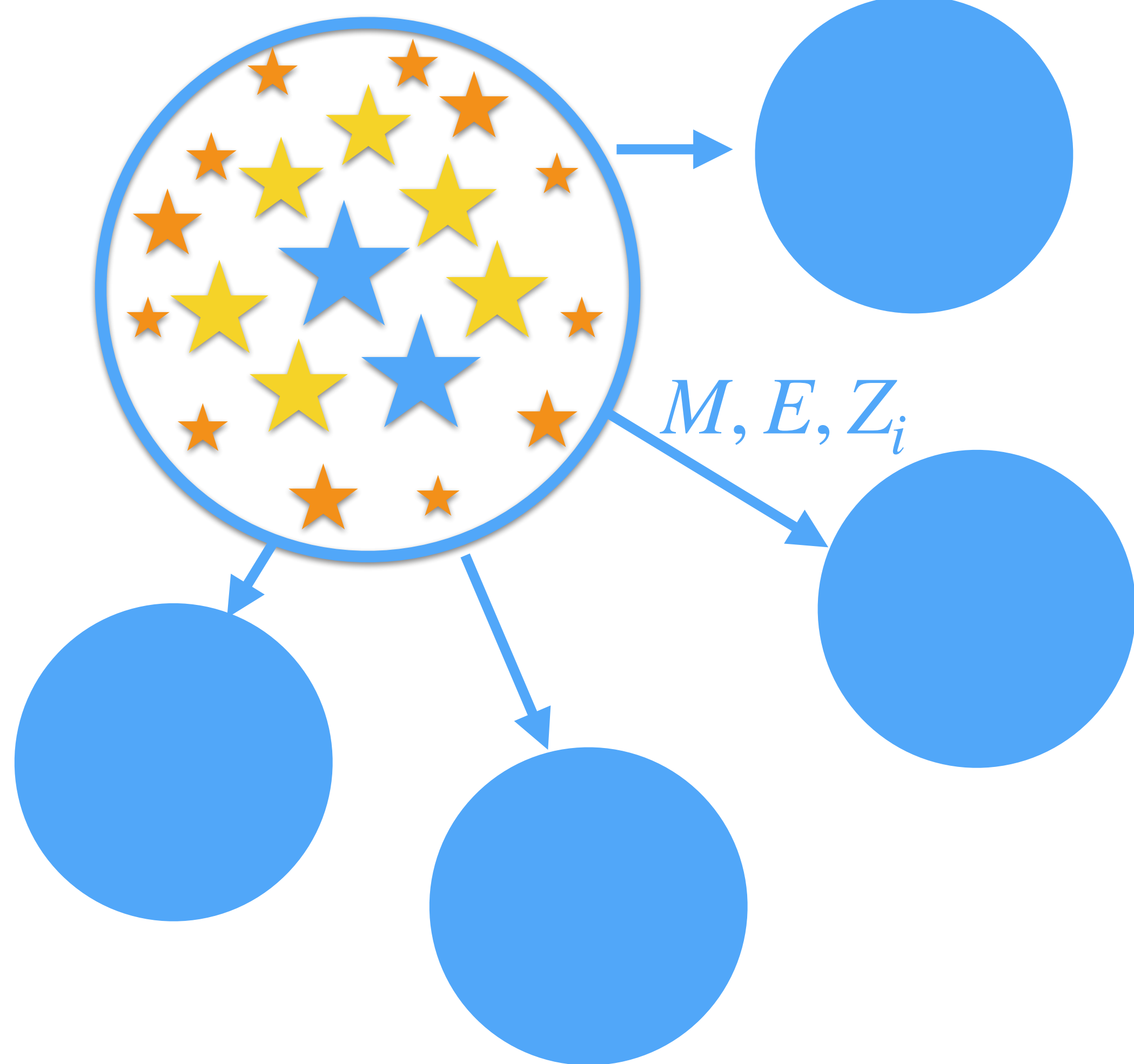


Simple stellar population



Chemical composition of mass return

nucleosynthetic yield tables for element production inside stars



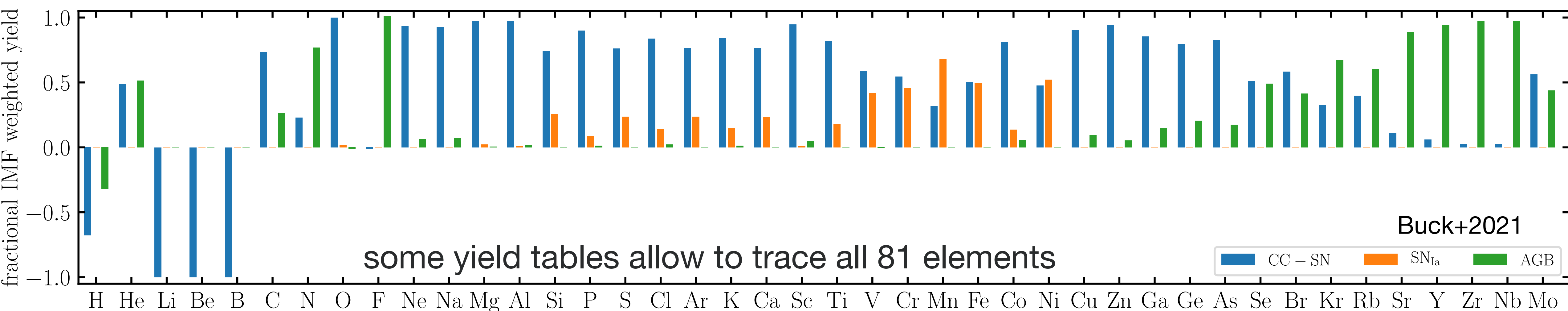
Yield Table	Masses	Metallicities
CC SN		
Portinari et al. (1998)	[6,120]	[0.0004,0.05]
François et al. (2004)	[11,40]	[0.02]
Chieffi & Limongi (2004)	[13,35]	[0,0.02]
Nomoto et al. (2013)	[13,40]	[0.001,0.05]
Frischknecht et al. (2016)	[15,40]	[0.00001,0.0134]
West & Heger (in prep.)	[13,30]	[0,0.3]
Ritter et al. (2018b)	[12,25]	[0.0001,0.02]
Limongi & Chieffi (2018) ^a	[13,120]	[0.00001,0.0134]
SN _{Ia}		
Iwamoto et al. (1999)	[1.38]	
Thielemann et al. (2003)	[1.374]	[0.02]
Seitenzahl et al. (2013)	[1.40]	[0.02]
AGB		
Karakas (2010)	[1,6.5]	[0.0001,0.02]
Ventura et al. (2013)	[1,6.5]	[0.0001,0.02]
Pignatari et al. (2016)	[1.65,5]	[0.01,0.02]
Karakas & Lugaro (2016)	[1,8]	[0.001,0.03]
TNG ^b	[1,7.5]	[0.0001,0.02]
Hypernova		
Nomoto et al. (2013)	[20,40]	[0.001,0.05]
		Buck+2021

17 yield tables

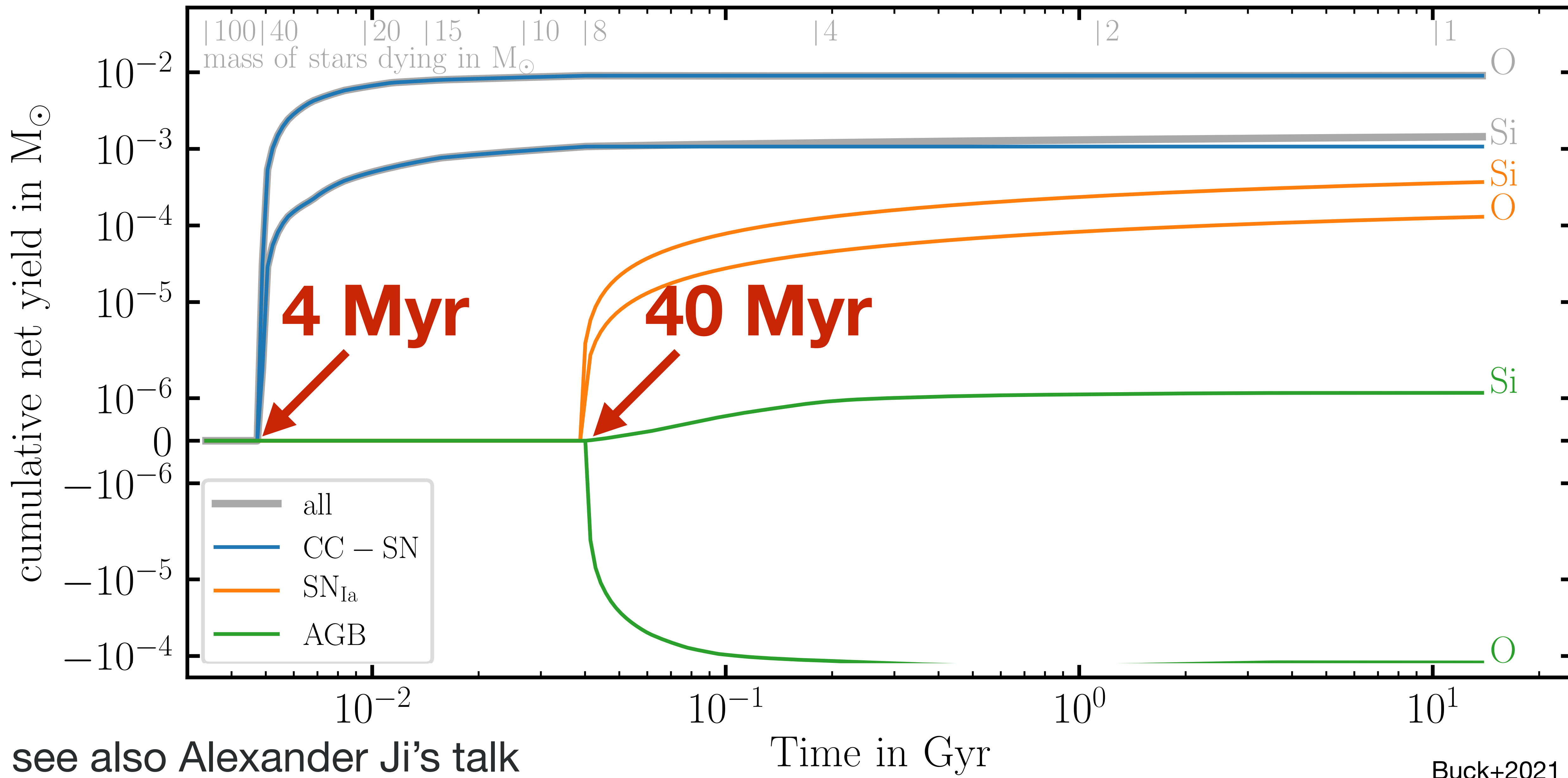


The importance of tracing cc-SN, SNIa and AGB enrichment

Importance of tracing a large set of elements



Time release of newly produced elements



Simulation Physics

Simulation Physics in Gasoline2

1

GASOLINE2 smooth particle hydrodynamics

„modern“ implementation of hydrodynamics,
metal diffusion

Wadsley+2017, Keller+2014

2

gas cooling

via hydrogen, helium and various metal lines

gas heating

via Photoionisation (e.g. from the UV background)

Shen+2010, Haardt&Madau 2012

3

self consistent star formation from cold, dense gas

Stinson+2006

star formation regions

$z = -0.00$

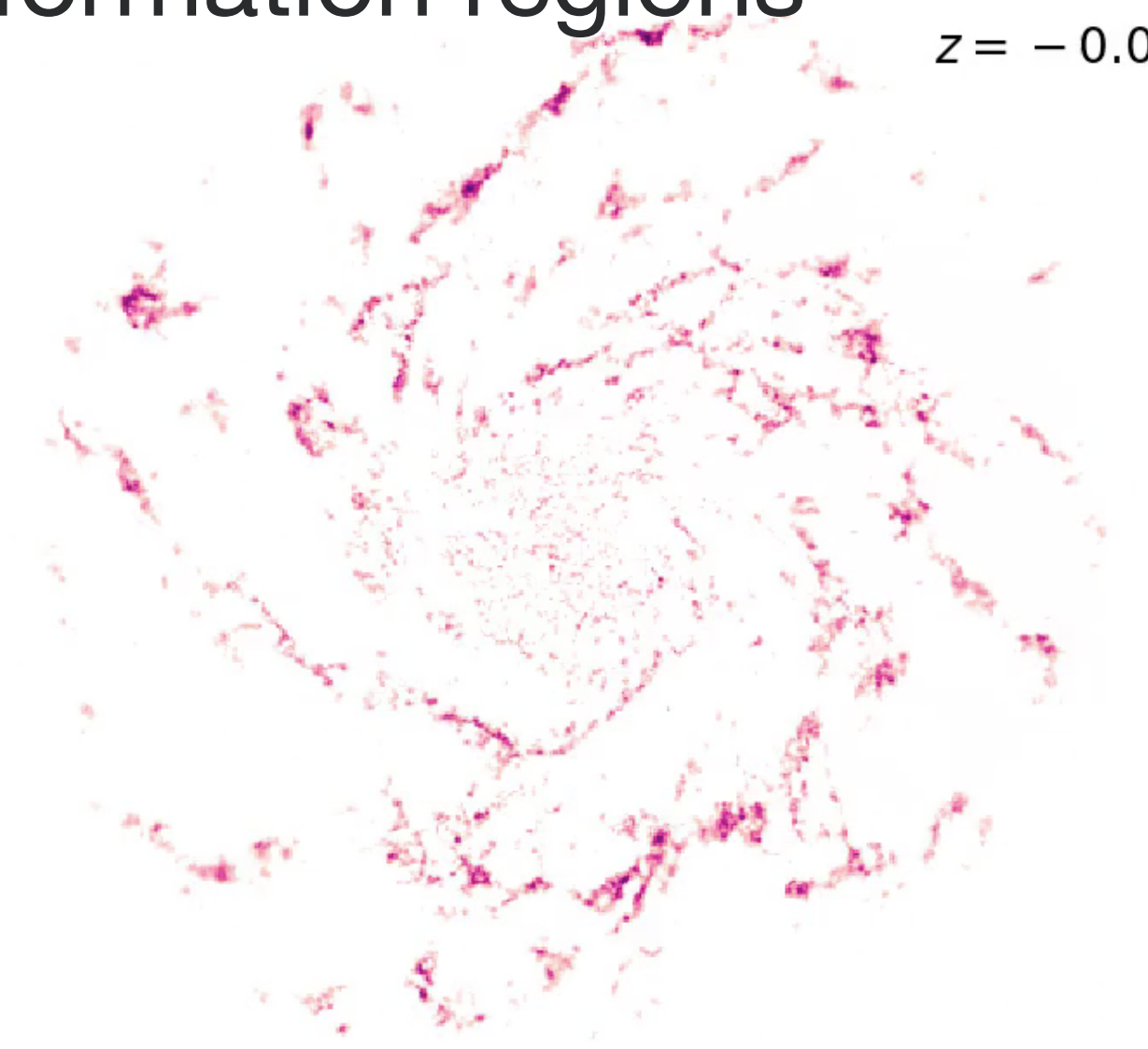


image size: 50x50 kpc

Animation by T. Buck (MPIA, NYUAD) based on NIHAO simulations

Buck+2019a

4

energetic feedback from young massive stars and supernovae

Stinson+2013

Simulation Physics in Gasoline2

1

GASOLINE2 smooth particle hydrodynamics

„modern“ implementation of hydrodynamics,
metal diffusion

Wadsley+2017, Keller+2014

2

gas cooling

via hydrogen, helium and various metal lines

gas heating

via Photoionisation (e.g. from the UV background)

Shen+2010, Haardt&Madau 2012

3

self consistent star formation from cold, dense gas

Stinson+2006

star formation regions

$z = -0.00$

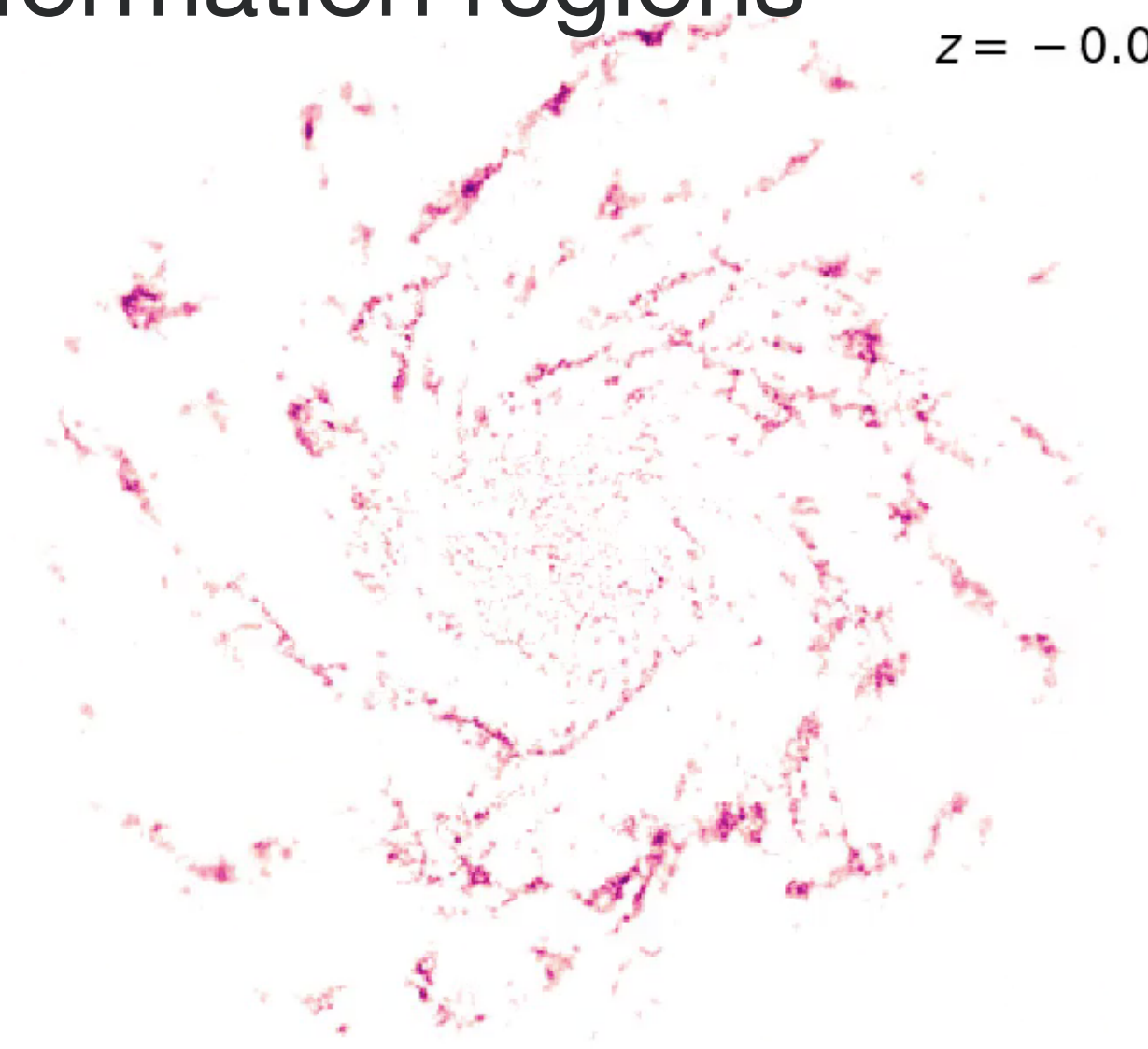


image size: 50x50 kpc

Animation by T. Buck (MPIA, NYUAD) based on NIHAO simulations

Buck+2019a

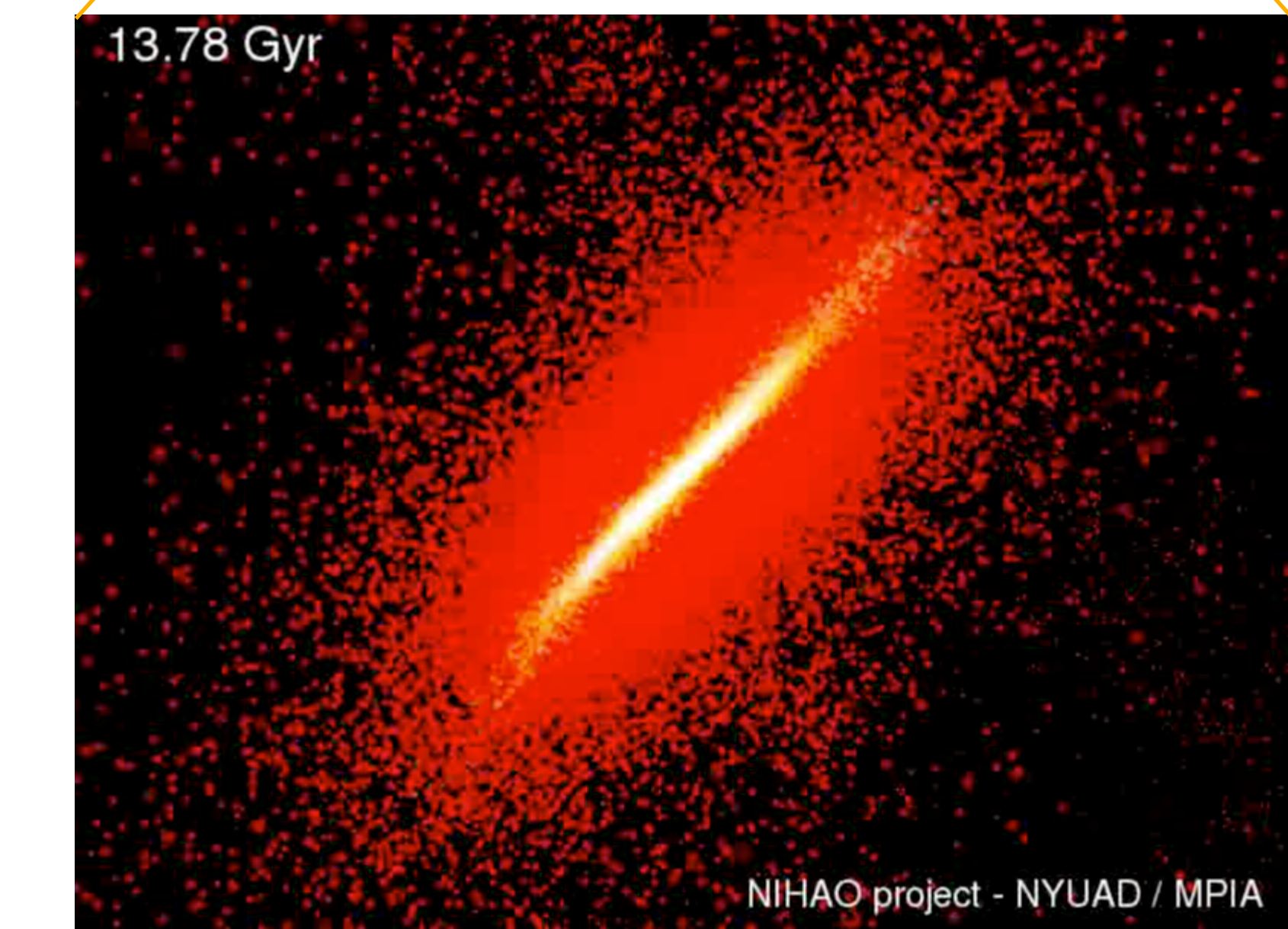
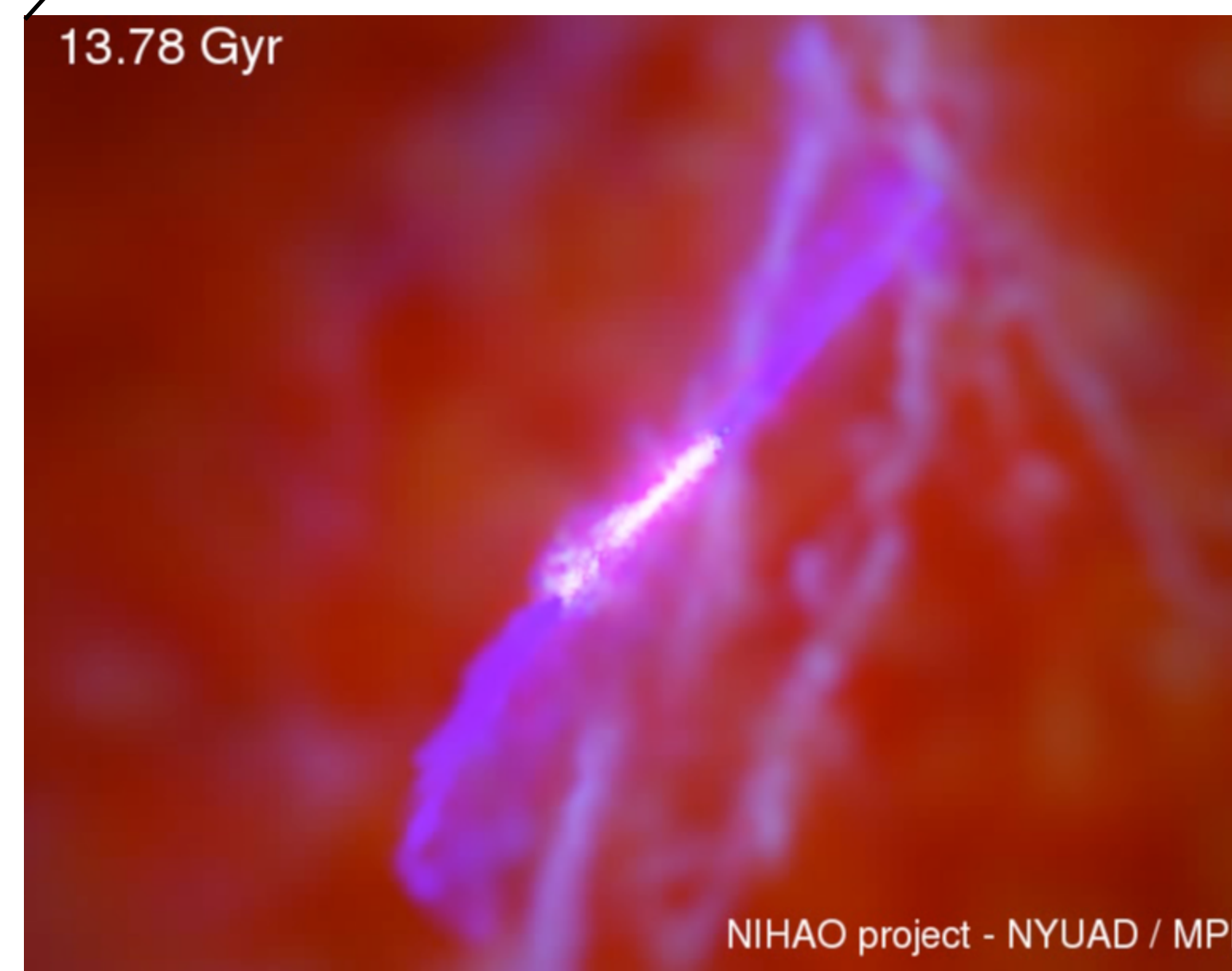
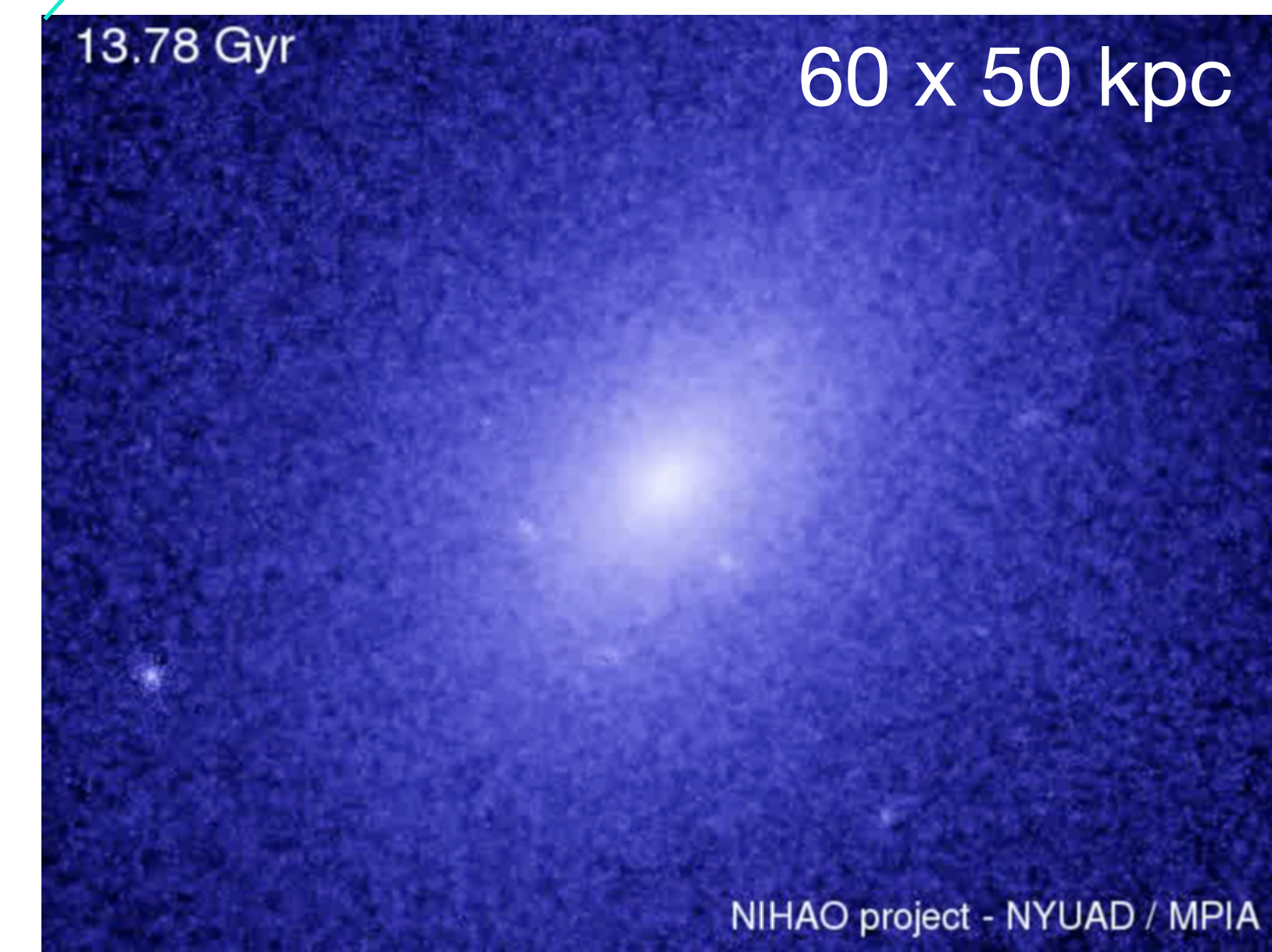
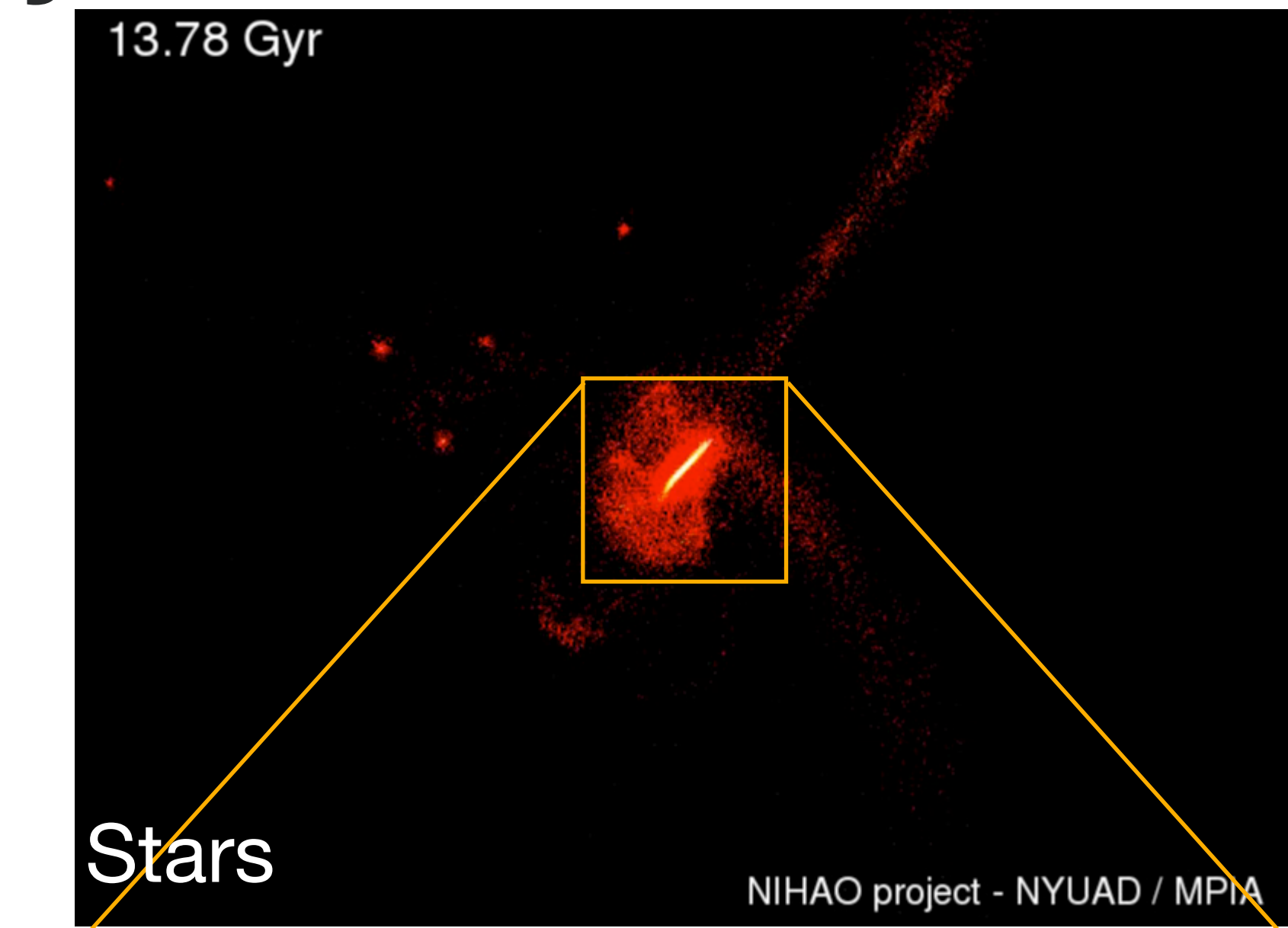
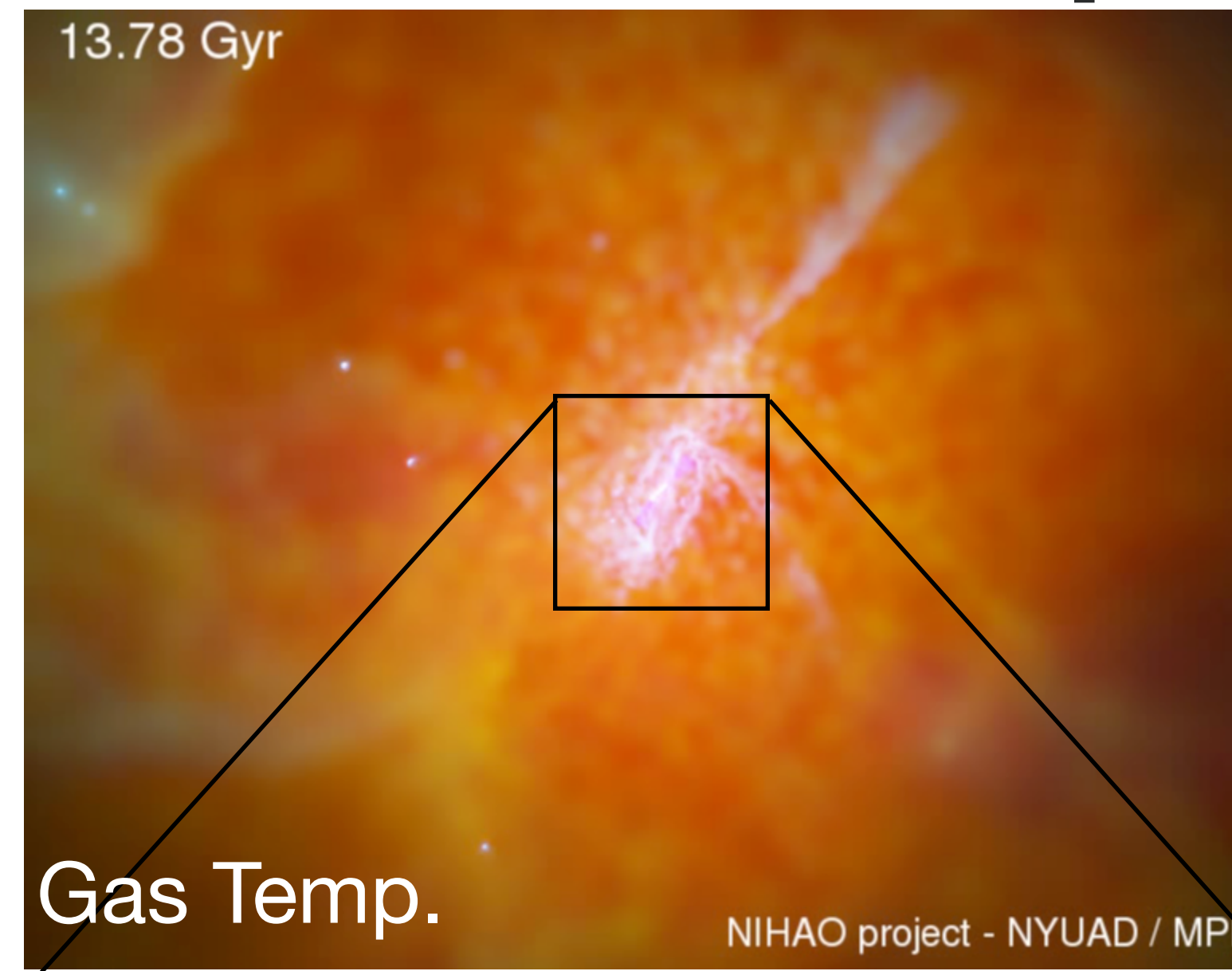
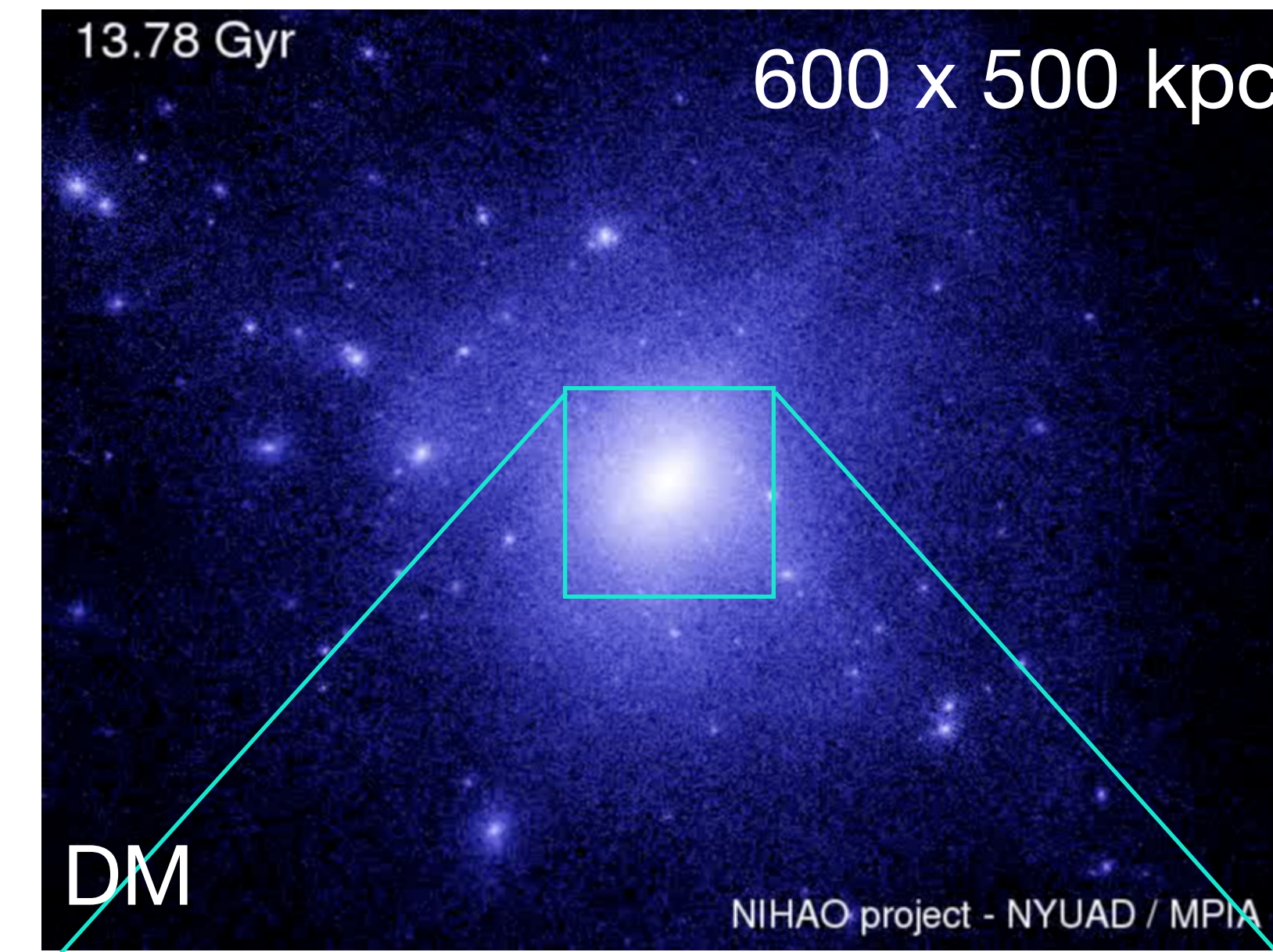
4

energetic feedback from young massive stars and supernovae

Stinson+2013

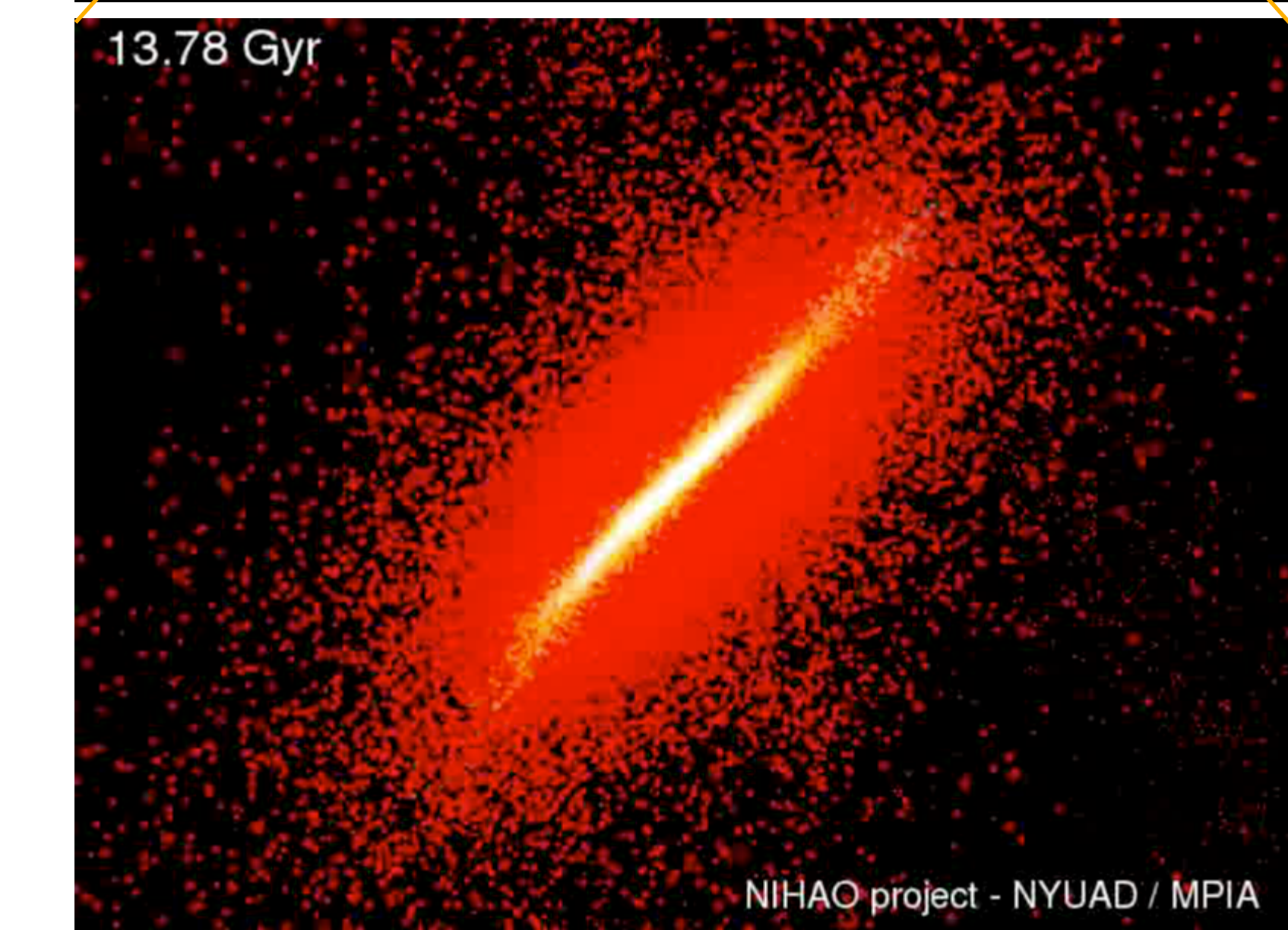
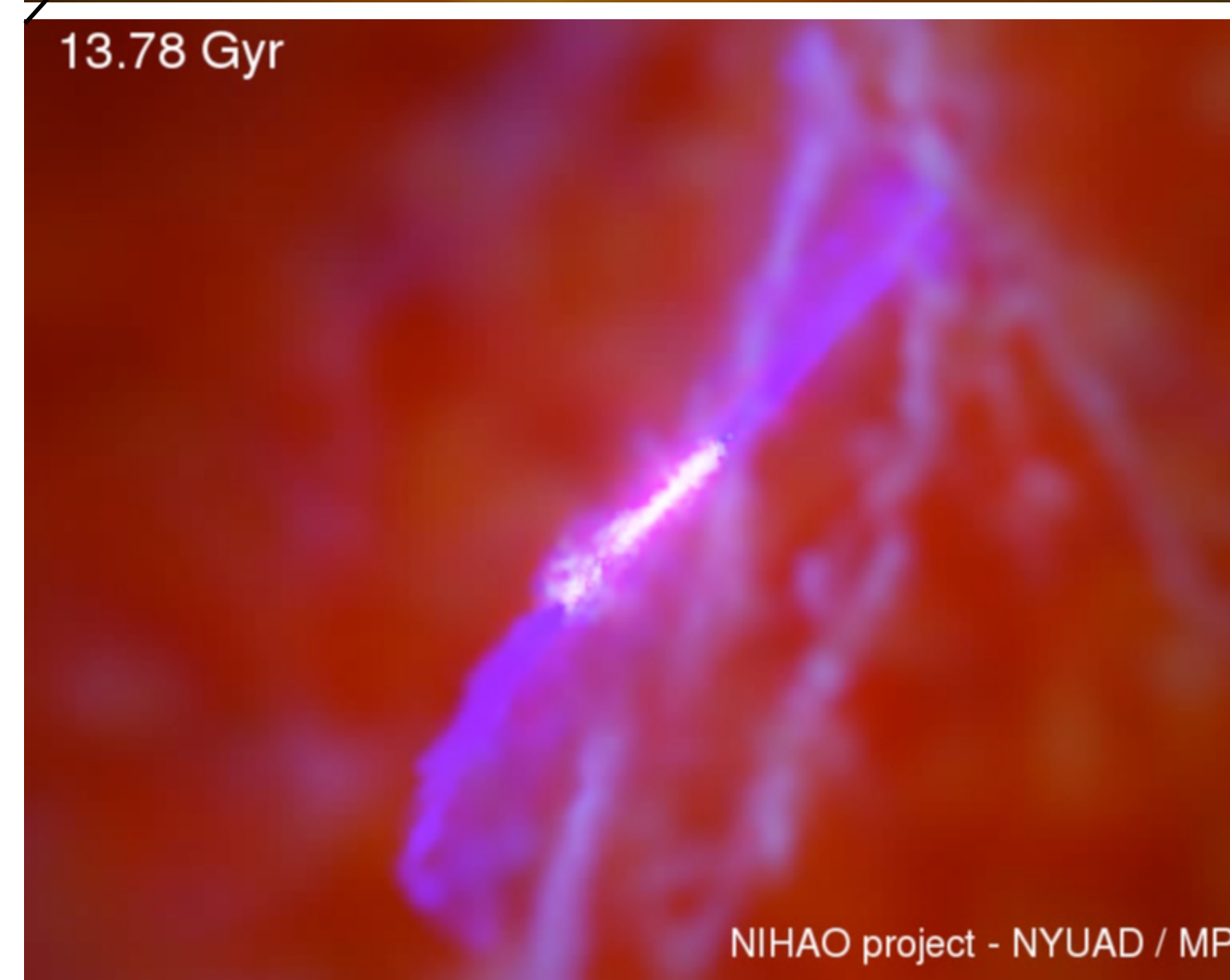
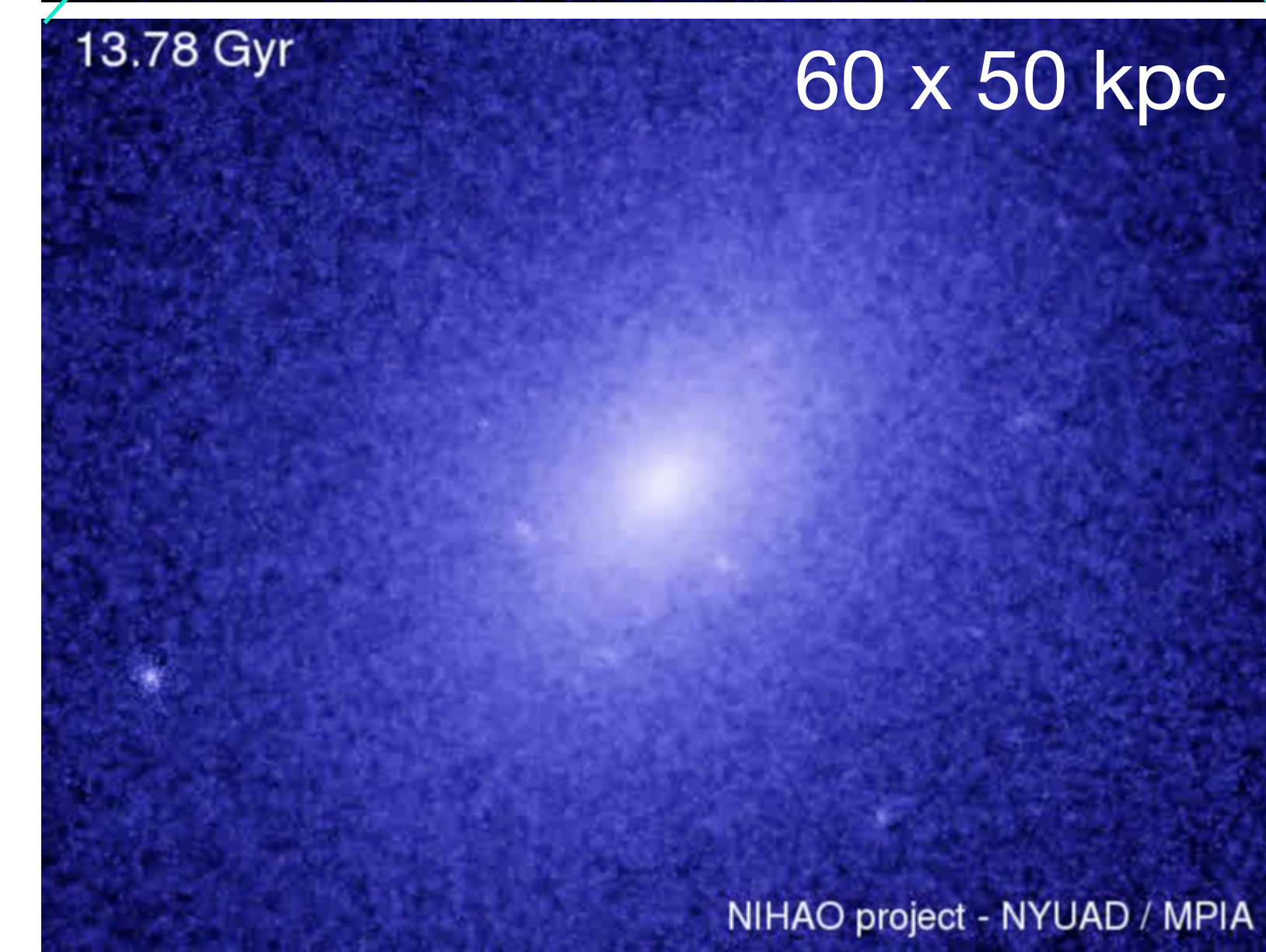
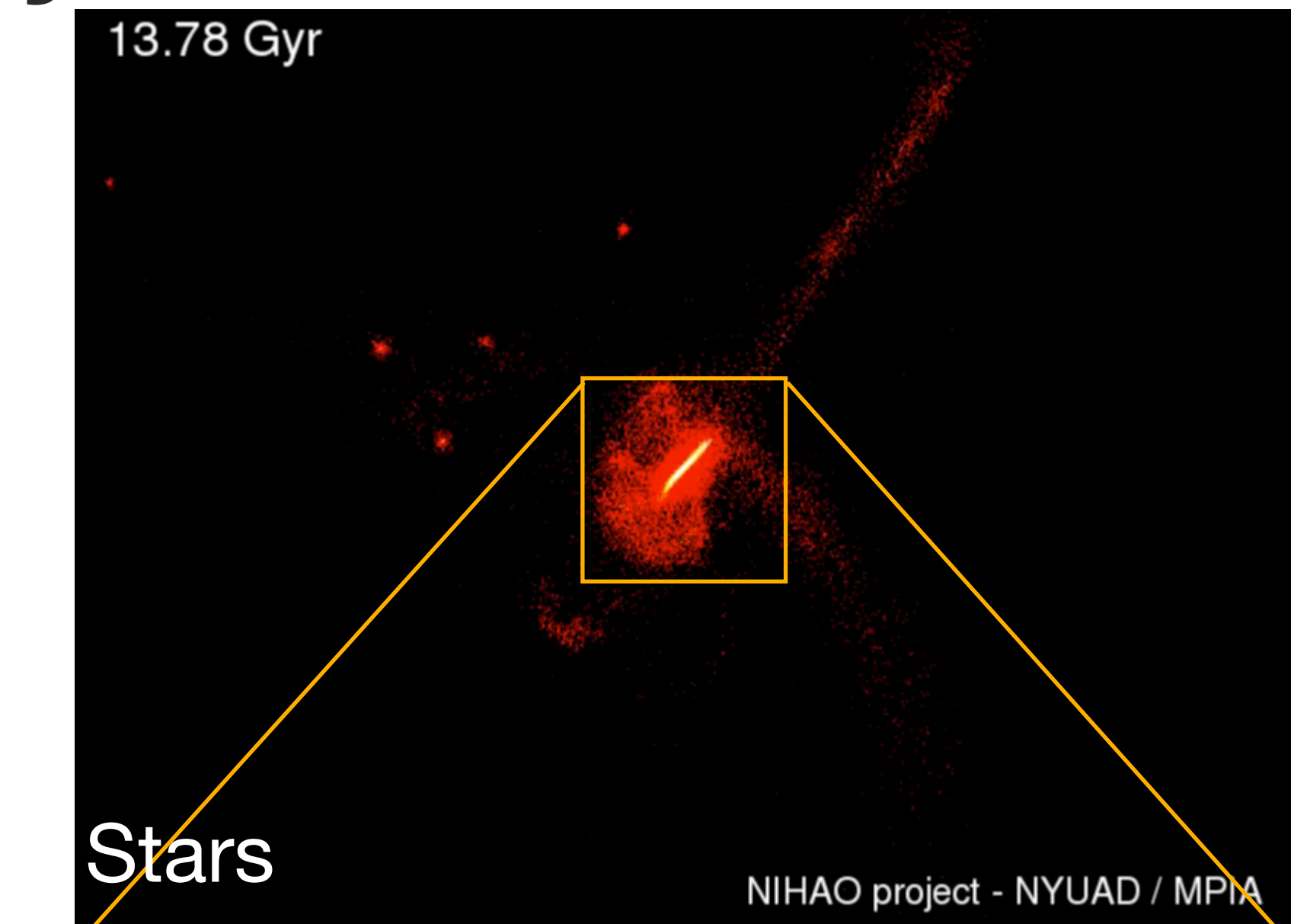
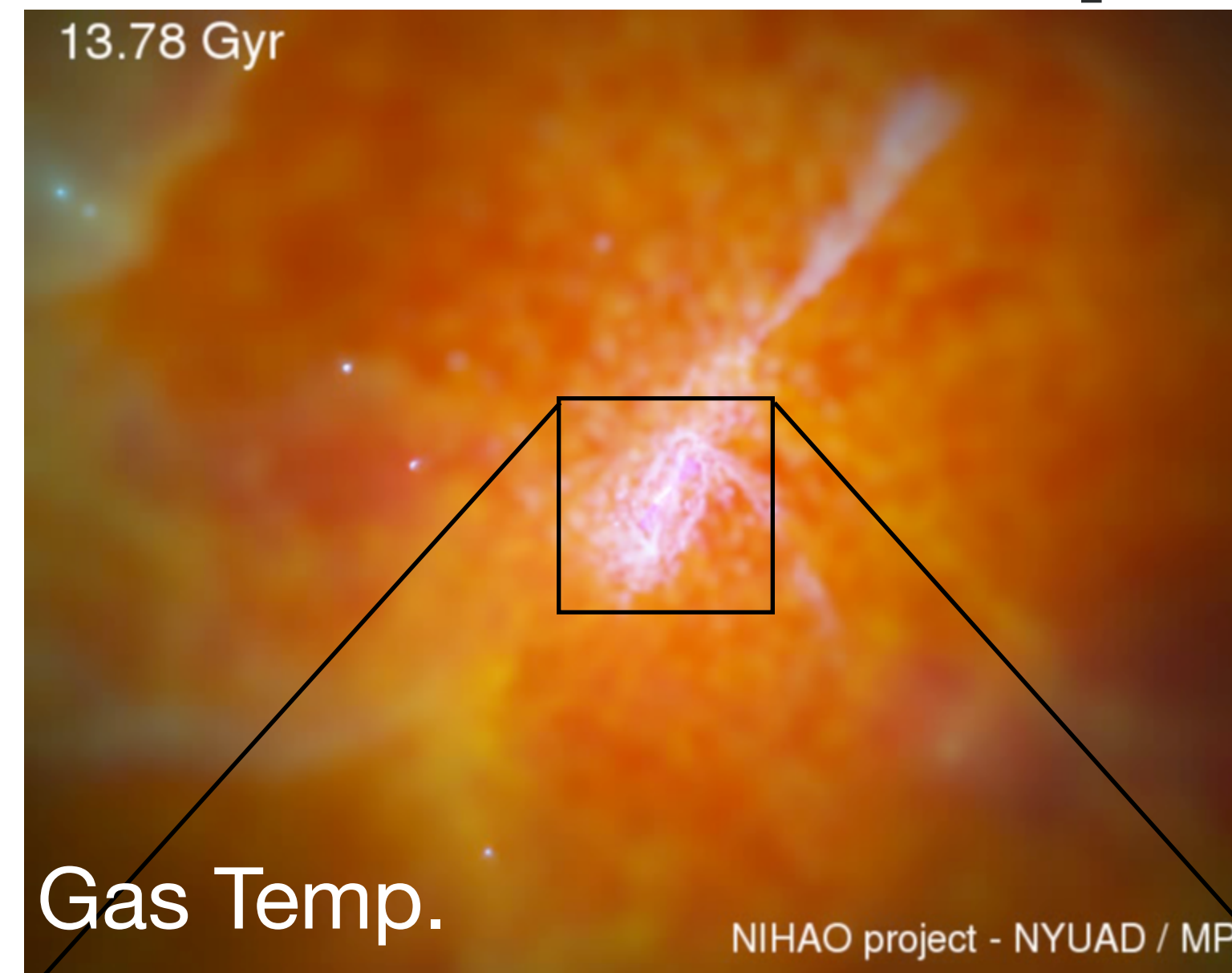
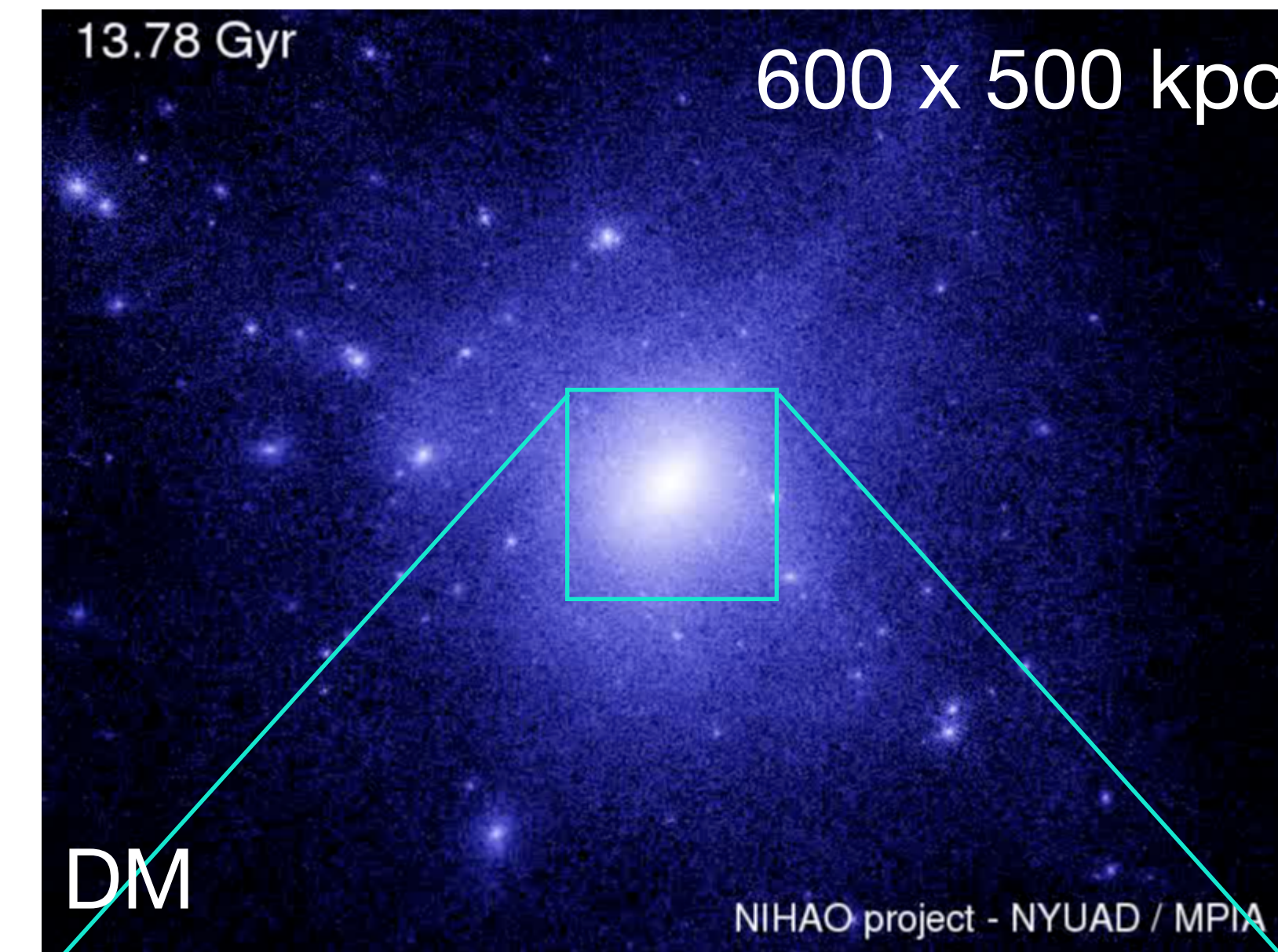
Formation of a simulated MW analogue in the NIHAO-UHD project

Buck+2019, Buck+2020



Formation of a simulated MW analogue in the NIHAO-UHD project

Buck+2019, Buck+2020

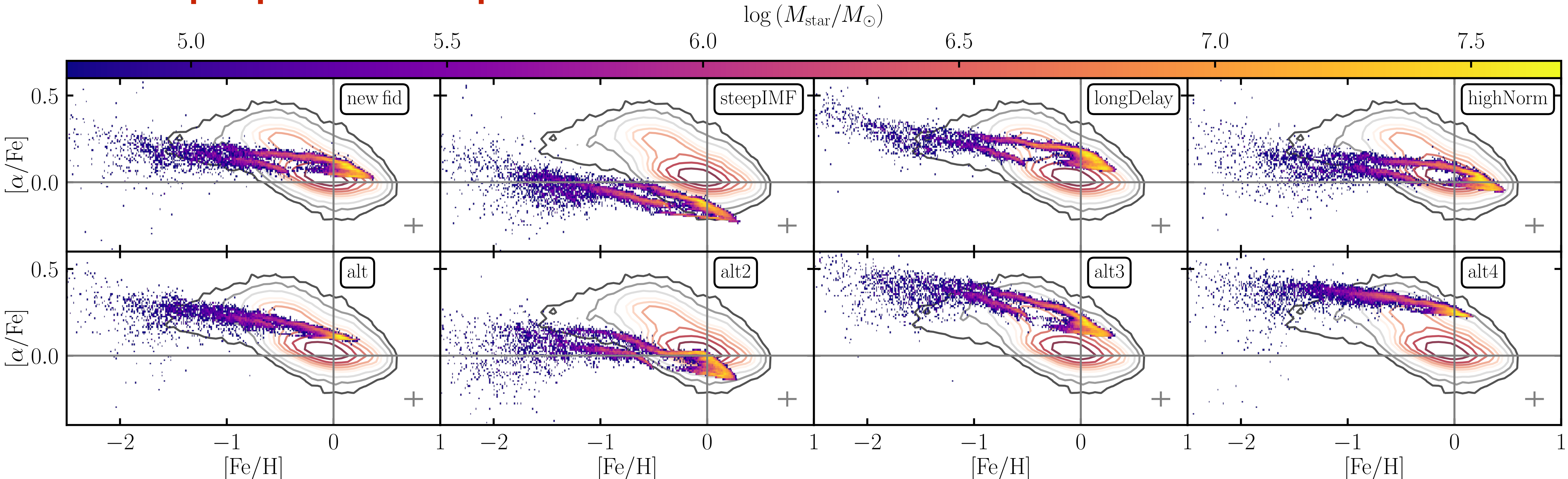




Results:
How do model assumptions
impact the results?

Systematic differences in $[\alpha/\text{Fe}]$ vs. $[\text{Fe}/\text{H}]$

Stellar population parameters



CC-SN yields

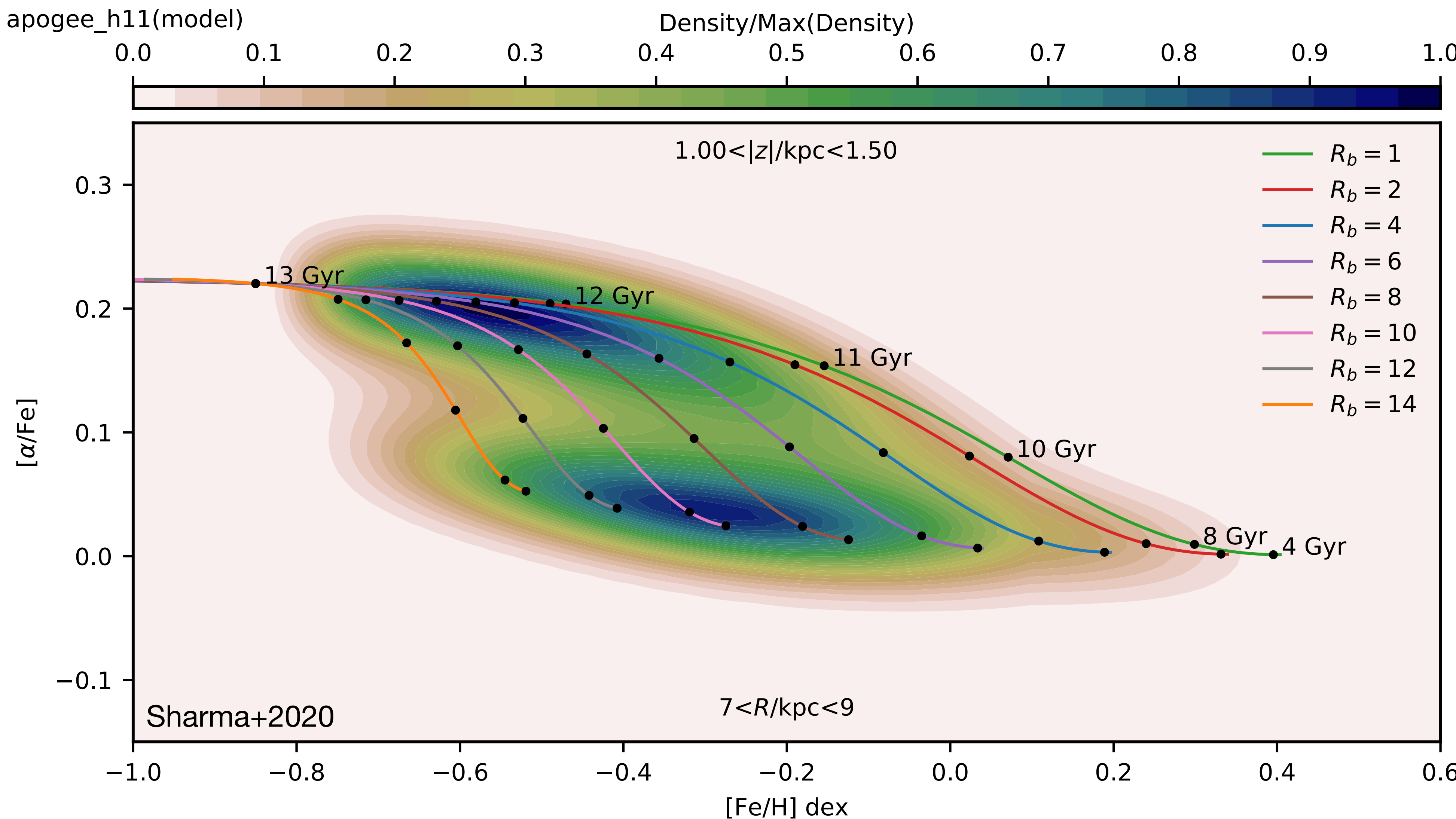
contours: Galah DR3

For differences in $[\text{X}/\text{Fe}]$ vs. $[\text{Fe}/\text{H}]$ see Buck+2021

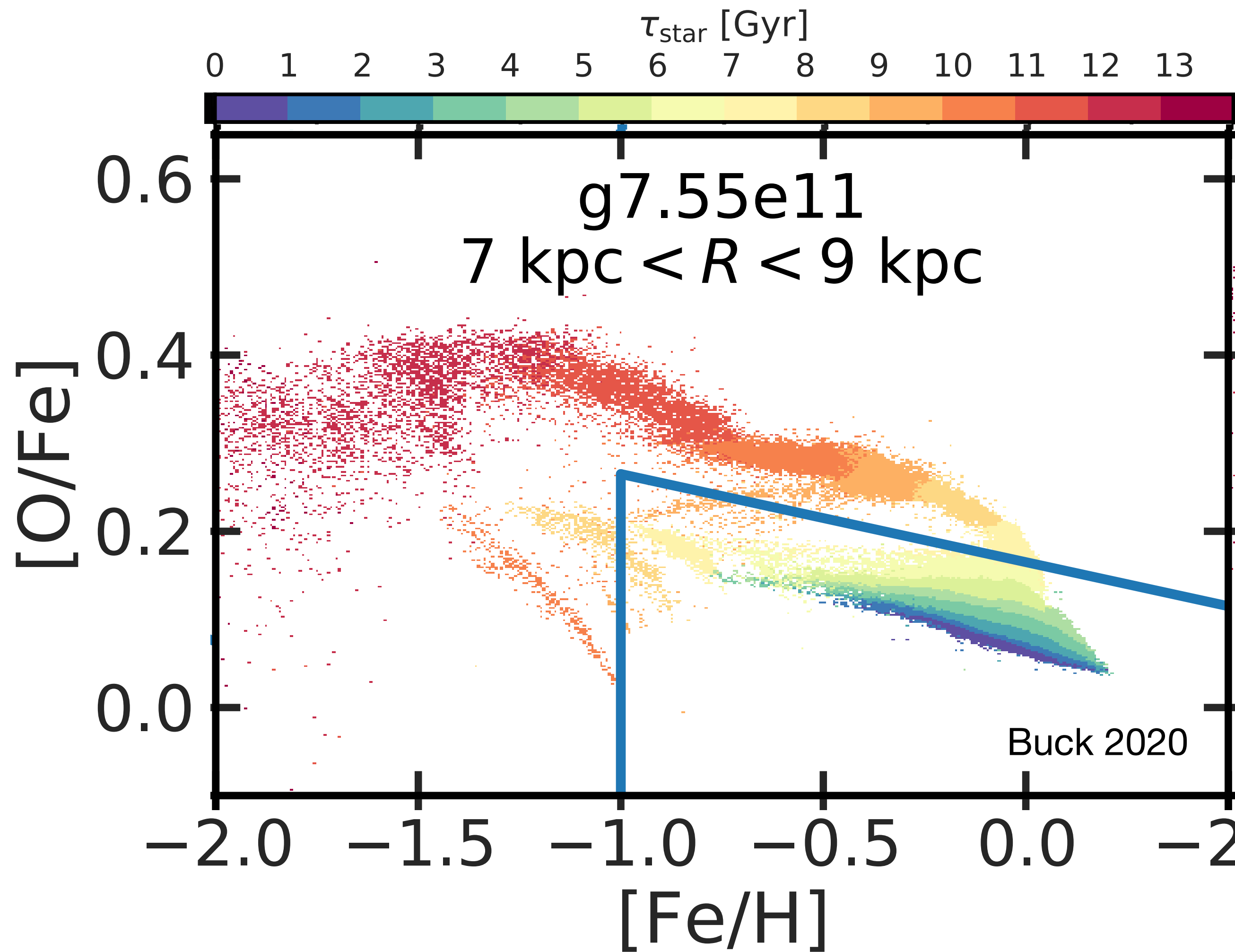
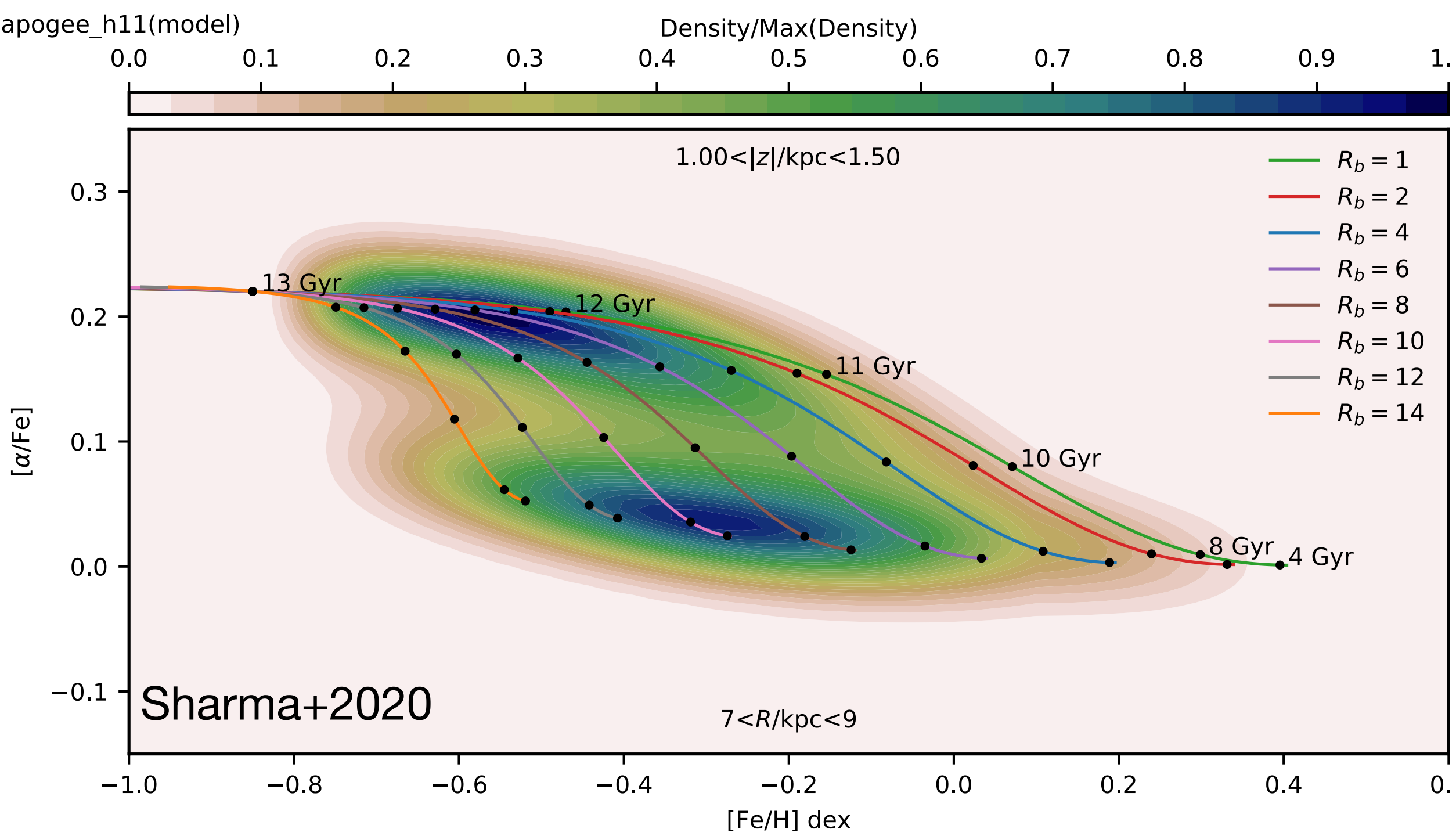


**What do we learn about the
formation of our
Milky Way?**

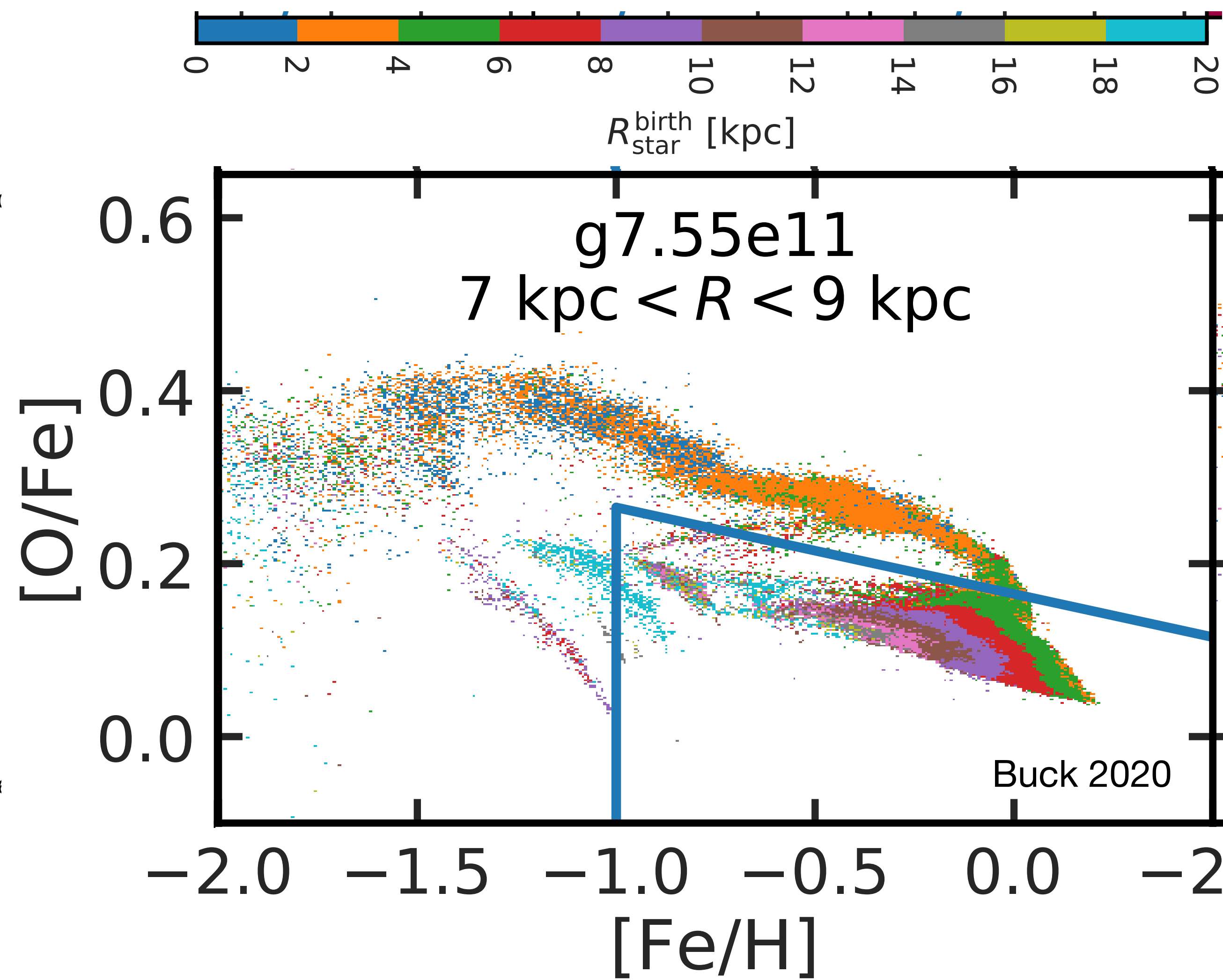
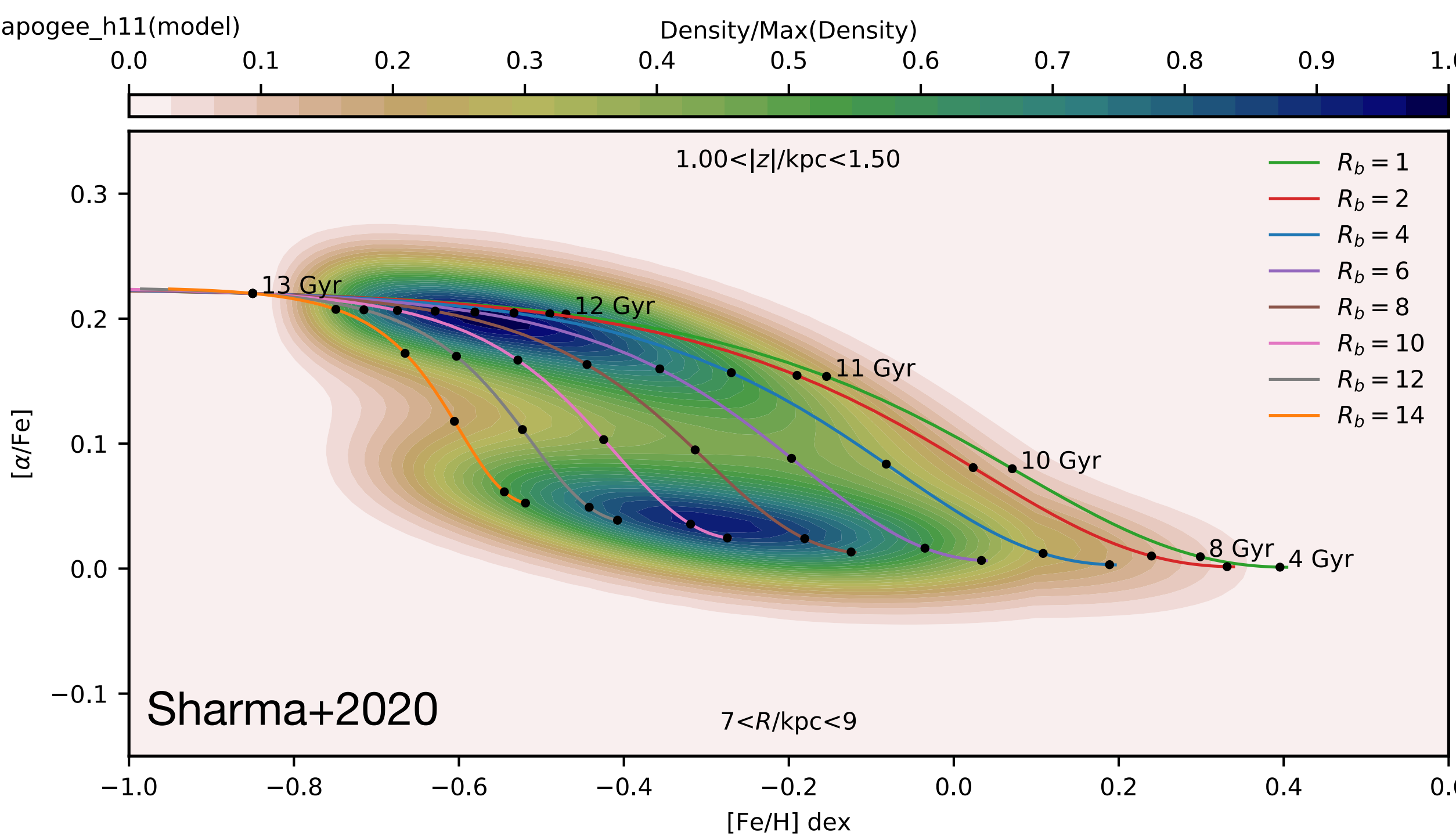
Formation of the bimodality in $[\alpha/\text{Fe}]$ vs. $[\text{Fe}/\text{H}]$ in analytic models

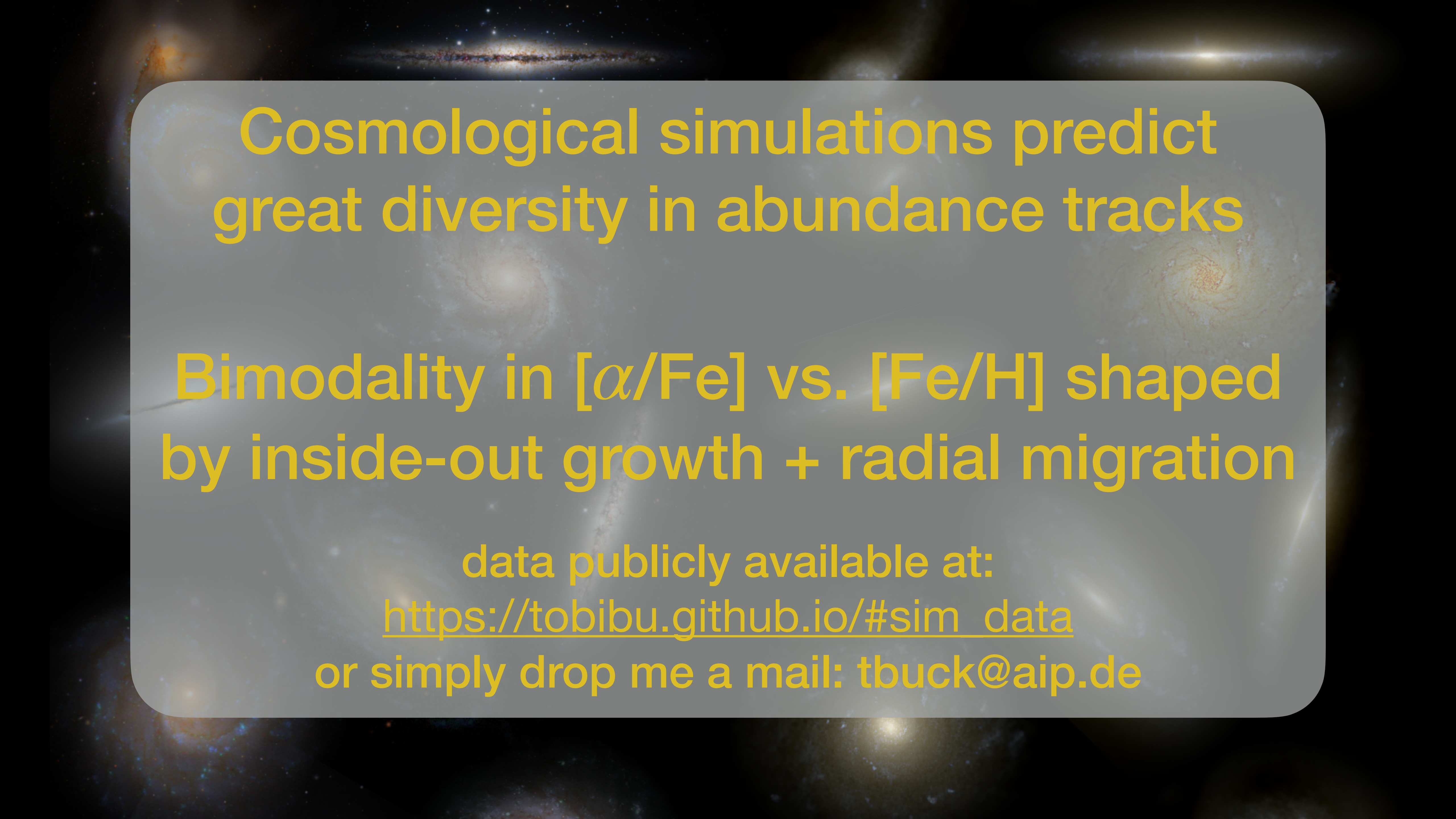


Formation of the bimodality in $[\alpha/\text{Fe}]$ vs. $[\text{Fe}/\text{H}]$ in cosmological simulations



Formation of the bimodality in $[\alpha/\text{Fe}]$ vs. $[\text{Fe}/\text{H}]$ in cosmological simulations





Cosmological simulations predict
great diversity in abundance tracks

Bimodality in $[\alpha/\text{Fe}]$ vs. $[\text{Fe}/\text{H}]$ shaped
by inside-out growth + radial migration

data publicly available at:

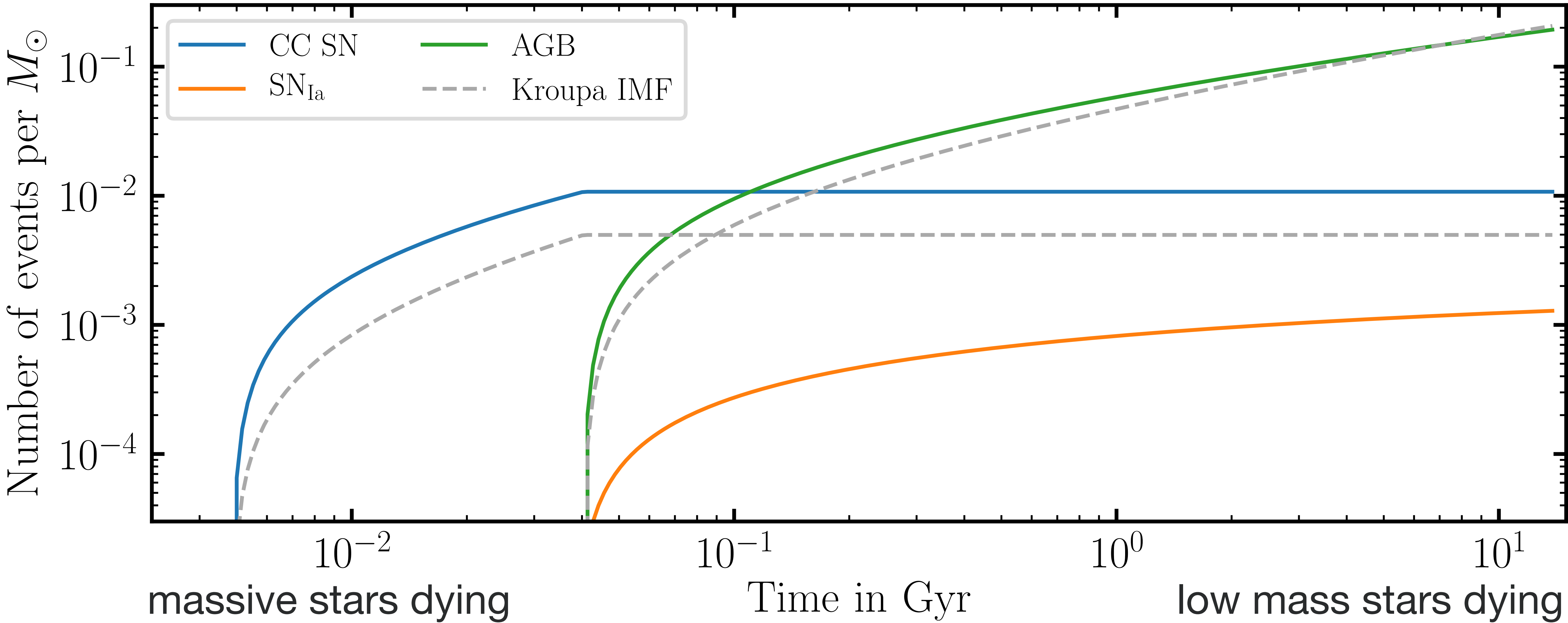
https://tobibu.github.io/#sim_data

or simply drop me a mail: tbuck@aip.de

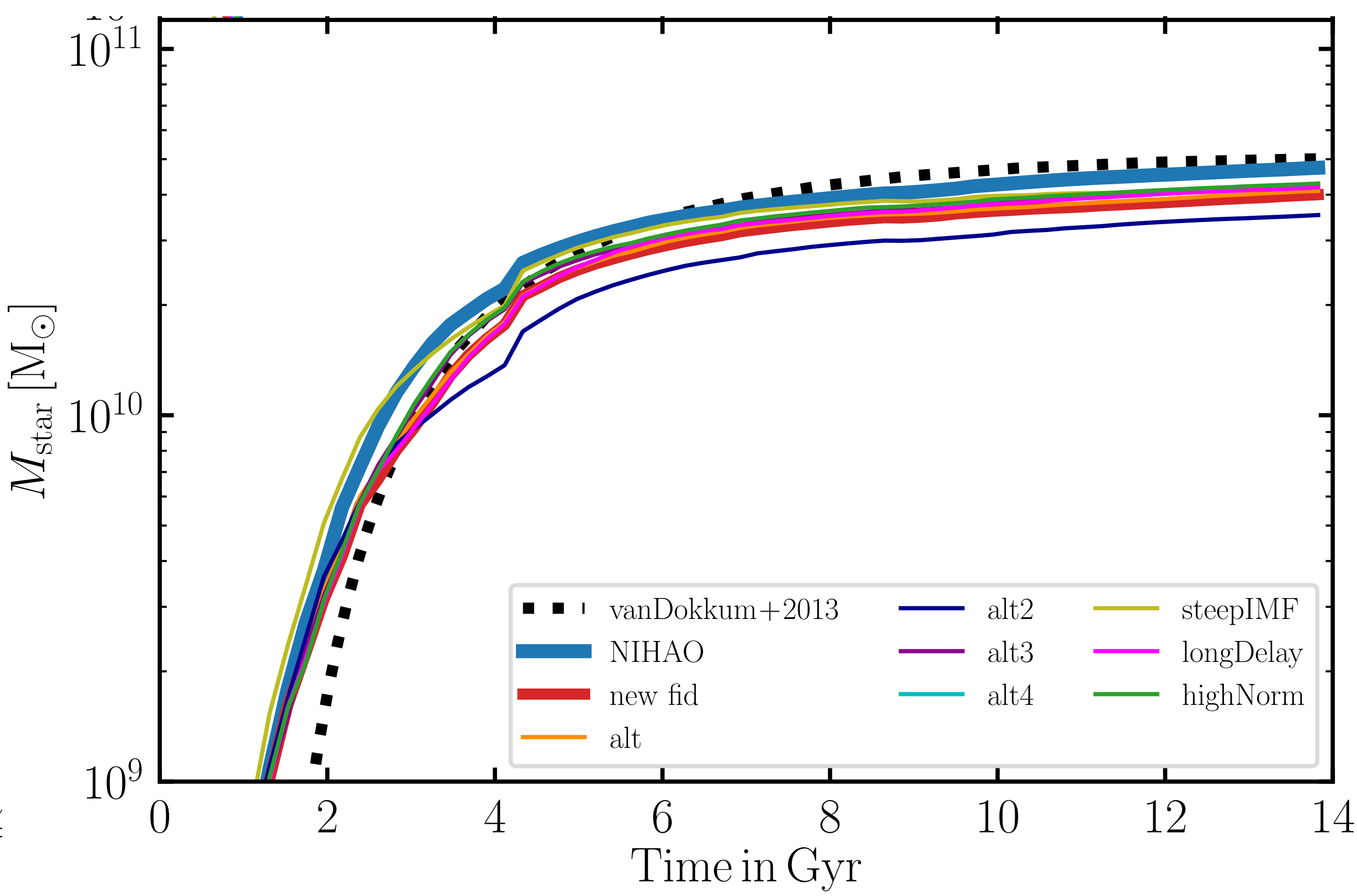
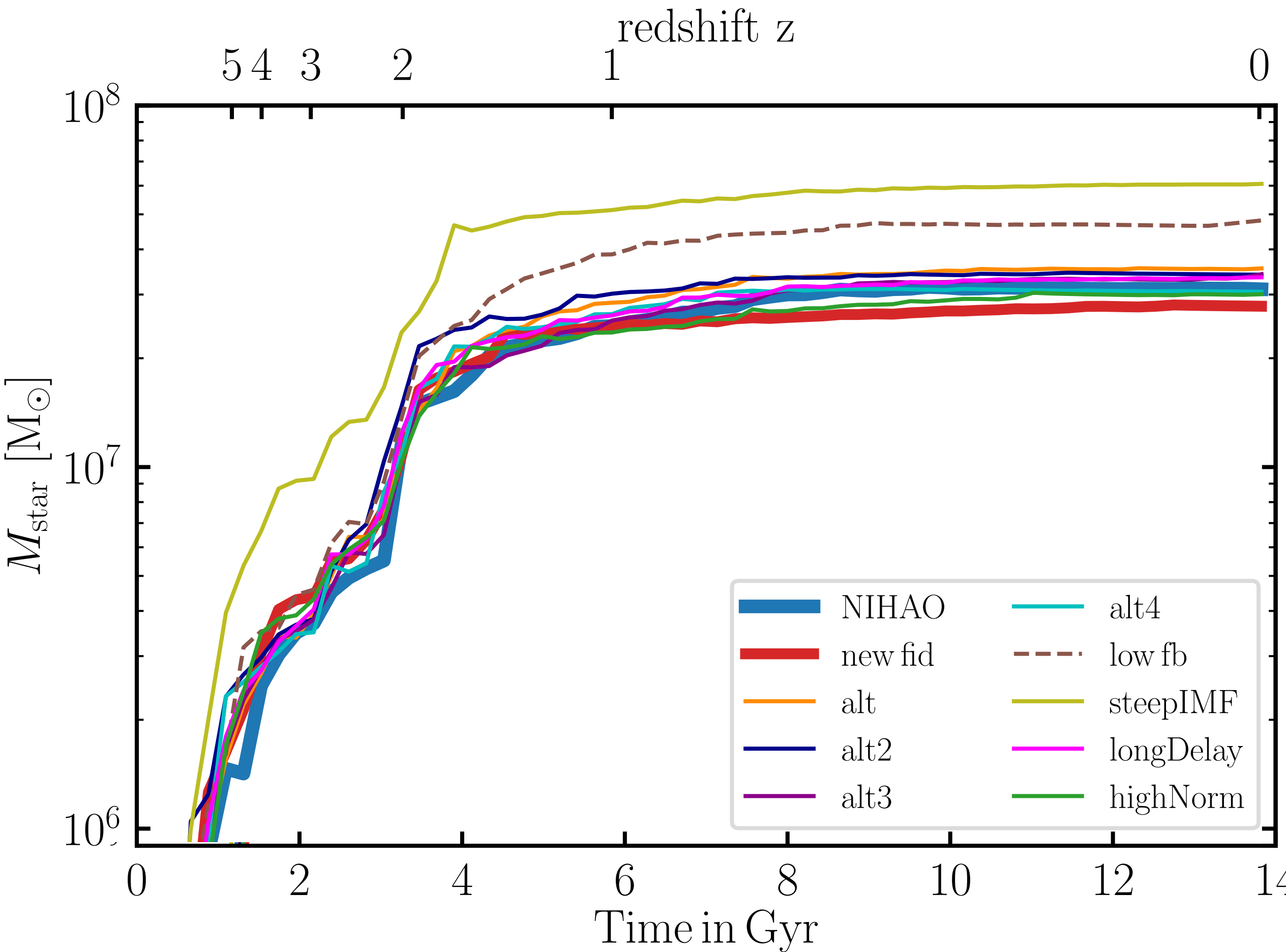
Simple stellar population model

assume mass ranges for CC-SN, AGB stars and SN Ia

here the number of SN Ia follows empirical delay time distribution



Star formation history



Buck subm.